



UNIVERSIDADE FEDERAL DE
UBERLÂNDIA



INSTITUTO DE CIÊNCIAS BIOMÉDICAS

Programa de Pós-Graduação em Imunologia e Parasitologia Aplicadas

**Interação entre uma metaloprotease purificada da peçonha de
Bothrops moojeni (BmooMP-alfa-I) e o fator de necrose tumoral
(TNF): modelos de estudo in vitro e in vivo.**

MARAISA CRISTINA SILVA

UBERLÂNDIA - MG

2017



UNIVERSIDADE FEDERAL DE
UBERLÂNDIA



INSTITUTO DE CIÊNCIAS BIOMÉDICAS

Programa de Pós-Graduação em Imunologia e Parasitologia Aplicadas

**Interação entre uma metaloprotease purificada da peçonha de
Bothrops moojeni (BmooMP-alfa-I) e o fator de necrose tumoral
(TNF): modelos de estudo in vitro e in vivo.**

Tese apresentada ao Colegiado do Programa de Pós-Graduação em Imunologia e Parasitologia Aplicadas da Universidade Federal de Uberlândia como parte dos requisitos para obtenção do título de Doutor.

ORIENTADOR: PROF. DR. JOSÉ ROBERTO MINEO

UBERLÂNDIA – MG
2017

Dados Internacionais de Catalogação na Publicação (CIP)
Sistema de Bibliotecas da UFU, MG, Brasil.

S586i Silva, Maraisa Cristina, 1985
2017 Interação entre uma metaloprotease purificada da peçonha de Bothrops moojeni (BmooMP-alfa-I) e o fator de necrose tumoral (TNF): modelos de estudo in vitro e in vivo / Maraisa Cristina Silva. - 2017.
58 p.

Orientador: José Roberto Mineo.

Tese (doutorado) - Universidade Federal de Uberlândia, Programa de Pós-Graduação em Imunologia e Parasitologia Aplicadas.

Disponível em: <http://dx.doi.org/10.14393/ufu.te.2018.18>

Inclui bibliografia.

1. Imunologia - Teses. 2. Bothrops - Teses. 3. Citocinas - Teses. 4. Fator de necrose tumoral alfa - Teses. I. Mineo, José Roberto. II. Universidade Federal de Uberlândia. Programa de Pós-Graduação em Imunologia e Parasitologia Aplicadas. III. Título.

CDU: 612.017

Angela Aparecida Vicentini Tzi Tziboy – CRB-6/947



Programa de Pós-graduação em Imunologia e Parasitologia Aplicada

Ata da defesa de Tese de Doutorado junto ao Programa de Pós-graduação em Imunologia e Parasitologia Aplicadas do Instituto de Ciências Biomédicas da Universidade Federal de Uberlândia.

Defesa da Tese de Doutorado número 97 do PPIPA.

Data: 28 de junho de 2017

Discente: MARAISA CRISTINA SILVA

Matrícula: 11313IPA004

Título do Trabalho: "Interação entre uma metaloprotease purificada da peçonha de *Bothrops moojeni* (BmooMP-alfa-I) e o fator de necrose tumoral (TNF): modelos de estudo in vitro e in vivo".

Área de concentração: Imunologia e Parasitologia Aplicadas.

Linha de Pesquisa: Imunologia e Biologia Celular de Patógenos Causadores de Doenças Infecciosas e Parasitárias

Às 14 horas do dia 28 de junho do ano de 2017 no Anfiteatro do Bloco 4K - Campus Umuarama da Universidade Federal de Uberlândia reuniu-se a Comissão Julgadora, designada pelo Colegiado do Programa de Pós-graduação em Imunologia e Parasitologia Aplicadas, assim composta: Prof. Dr. Marcos Vinícius da Silva – UFTM, Prof. Dr. Odonório Abrahão Júnior – UFTM, Profa. Dra. Renata Santos Rodrigues – INGEB/UFU, Prof. Dr. João Marcos Madurro – IQ/UFU e Prof. Dr. José Roberto Mineo – ICBIM/UFU, orientador da candidata.


Iniciando os trabalhos o(a) presidente da banca Dr. José Roberto Mineo apresentou a comissão examinadora e o(a) candidato(a). Agradeceu a presença do público e concedeu ao(à) discente a palavra para exposição do seu trabalho. A duração da apresentação do(a) discente e o tempo de arguição e resposta foram conforme as normas do Programa.

A seguir o(a) senhor(a) presidente concedeu a palavra, pela ordem sucessivamente, aos examinadores, que passaram a arguir o candidato. Ultimada a arguição, que se desenvolveu dentro dos termos regimentais, a banca, em sessão secreta, atribuiu os conceitos finais.

Em face do resultado obtido, a banca examinadora considerou o(a) candidato(a) aprovado(a).

Esta defesa de tese é parte dos requisitos necessários à obtenção do título de doutor(a). O competente diploma será expedido após cumprimento dos demais requisitos, conforme as normas do Programa, legislação e regulamentação interna da UFU, e Conselho de Pós-graduação e Pesquisa desta Universidade.


Nada mais havendo a tratar foram encerrados os trabalhos às 18 horas e 17 minutos. Foi lavrada a presente ata que após lida e achada conforme foi assinada pela banca examinadora.


Prof. Dr. Marcos Vinícius da Silva
UFTM


Prof. Dr. Odonório Abrahão Júnior
UFTM


Profa. Dra. Renata Santos Rodrigues
INGEB/UFU


Prof. Dr. João Marcos Madurro
IQ/UFU


Prof. Dr. José Roberto Mineo – orientador
ICBIM/UFU

Em um momento muito delicado da minha vida pessoal e rodeada de obstáculos concluo mais uma parte deste trabalho ao qual venho me dedicando há anos... E se hoje vocês o leem é porque **DEUS** me sustentou e permitiu que concluísse essa etapa...

“Sou grato pela vida;

Agradeço pelo ar que entra em meus pulmões e que me traz a vida.;

Agradeço pelo sol que me esquenta;

Manifesto uma profunda gratidão pela água que chega até minha casa;

Sou grata por cada dia que me traz uma nova oportunidade de ser feliz;

Expresso a gratidão por cada pessoa que passa em minha vida;

Agradeço por todas as coisas boas que acontecem em meu dia;

Expresso uma profunda gratidão por todas as coisas que tenho;

Agradeço por ter conhecido as pessoas que amo;

Agradeço por ter conhecido as pessoas que tive algum desentendimento, pois elas acabaram sendo professores de minha vida espiritual e emocional.

Agradeço pela noite que me permite descansar e recarregar minhas energias;

Sou grato por minha cama que me proporciona uma boa noite de sono;

Sou grato por todas as coisas simples que tenho e que sem elas minha vida seria muito difícil...

Minha gratidão e dedicatória hoje e sempre ao Altíssimo... Abba...Yavé...

Há um lugar de descanso em Ti
Há um lugar de refrigério em Ti
Há um lugar onde a verdade reina
Esse lugar é no Senhor

Há um lugar onde as pessoas não me influenciam
Há um lugar onde eu ouço teu Espírito
Há um lugar de vitória em meio à guerra
Esse lugar é no Senhor

Esse lugar é no Senhor
Esse lugar é no Senhor
Esse lugar é no Senhor
Esse lugar é no Senhor

Há um lugar onde a inconstância não me domina
Há um lugar onde minha fé é fortalecida
Há um lugar onde a paz é quem governa
Esse lugar é no Senhor

Há um lugar onde os sonhos não se abortam
Há um lugar onde os seus medos não te dominam
Há um lugar que quando se perde é que se ganha
Esse lugar é no Senhor

Jesus
Tu és tudo o que eu preciso, Jesus!
Eu te preciso...

Há um lugar
(Heloísa Rosa)

Agradecimentos

A **DEUS** pela vida que me foi concedida, pelas oportunidades e conquistas alcançadas. Por me dar forças nos vários momentos difíceis e olhar pelo meu crescimento.

Aos meus pais, **ERCI e VANILDA**, vocês são a minha fonte de inspiração que ensinaram tudo de bom que aprendi em minha vida.

A você **MÃE** que me recebeu desde pequena com seu abraço caloroso e com sábias palavras me ensinou lutar pelos meus objetivos e, sempre com seu sorriso fácil e alegre me deu forças para continuar.

A você **PAI** pela proteção, carinho e principalmente por me ensinar a ter fé. Obrigada por me orientar em meu feito de lutas e incertezas, mas também de muitas esperanças e sonhos.

Aos meus irmãos, **CARLA e DOUGLAS**, com vocês que compartilho em minha vida tantos momentos bons de risadas, brincadeira, festas e, claro meus problemas.

Aos meus colegas do **LABORATÓRIO DE IMUNOPARASITOLOGIA**, pelo trabalho compartilhado, as dúvidas, o aprendizado, as brincadeiras que me fizeram sorrir. Obrigada principalmente pelo apoio nas horas difíceis, somente com ele e a amizade de vocês consegui chegar até aqui. Não citarei nomes para não cometer injustiça com ninguém todos vocês foram muito importantes pra mim e, hoje são meus amigos de coração.

Ao meu orientador, **Dr. JOSÉ ROBERTO MINEO**, por me receber como aluna, pela oportunidade de trabalho, pelo incentivo, por compreender minhas dificuldades, pelo apoio nos momentos de dúvidas. Foi ótimo caminhar ao lado da nossa equipe.

Aos **funcionários** do Programa de Pós-Graduação em Imunologia e Parasitologia, pela colaboração na resolução dos problemas e amizade.

Ao apoio financeiro dos órgãos de fomento a pesquisa: CAPES, CNPQ e FAPEMIG.

SUMÁRIO

RESUMO.....	1
ABSTRACT.....	2
APRESENTAÇÃO	3
CAPÍTULO I: SILVA, M.C et al. 2016.....	(Seção I)..6
CAPÍTULO II: SILVA, M.C et al. 2019	(Seção II)..31
CAPÍTULO III: PERPESCTIVAS FUTURAS.....	(Seção II)..52

RESUMO

A inflamação é um processo essencial para manutenção da homeostase, envolvendo eventos vasculares, migração e ativação de leucócitos. No entanto, suas manifestações exacerbadas, geralmente mediadas pelo aumento do nível de citocinas pró-inflamatórias como o fator de necrose tumoral (TNF), podem resultar em doenças crônicas, como artrite reumatóide, fibrose pulmonar e reações de hipersensibilidade. O presente estudo teve por objeto avaliar se a enzima BmooMP-alfa-I, uma metaloprotease isolada da peçonha de *Bothrops moojeni*, apresenta algum papel na resposta inflamatória em modelos experimentais *in vitro* e *in vivo*. Foi realizado o isolamento da enzima BmooMP- alfa -I, a partir da peçonha bruta da serpente *B. moojeni*, utilizando colunas de cromatografia DEAE Sephacel, Sephadex G-75 e Benzamidina-Sepharose. A eletroforese bidimensional (2D) demonstrou grau de pureza, massa molecular (*Mr*) e ponto isoelétrico (pI) em condições não redutoras somente um *spot* protéico pode ser evidenciado (~23,0 kDa; pI 6,82). Os níveis de TNF determinados pelo método de ELISA foram reduzidos significativamente na presença da enzima BmooMP-alfa-I, sugerindo que a mesma exerce uma ação proteolítica sobre o TNF, que foi confirmada pelo desaparecimento desta citocina dentre o perfil de bandas protéicas no SDS-PAGE e Western Blotting. O ensaio com macrófagos ativados com agonistas de PRRs, demonstrou uma redução níveis de TNF secretado pelos macrófagos após o seu tratamento com a enzima BmooMP-alfa-I. Estudos *in vivo* (ensaio do choque séptico e colite induzida por DSS) também mostraram que BmooMP-alfa-I é capaz de reduzir os níveis de TNF circulante e melhorar outros aspectos do quadro inflamatório intestinal. Em conclusão, a metaloprotease BmooMP-alfa-I apresenta um perfil antiinflamatório de reposta imunológica, resultante da sua ação direta sobre a citocina pró-inflamatória TNF.

Palavras-chaves: *Bothrops moojeni*, BmooMP-alfa-I, TNF

ABSTRACT

Inflammation is an essential process for maintaining homeostasis, involving vascular events, migration and activation of leukocytes. However, its exacerbated manifestations, usually mediated by increased levels of proinflammatory cytokines such as tumor necrosis factor (TNF), may result in chronic diseases such as rheumatoid arthritis, pulmonary fibrosis, and hypersensitivity reactions. The present study aimed to evaluate whether the enzyme BmooMP- α -I, a metalloprotease isolated from *Bothrops moojeni* venom, has some role in the inflammatory response in experimental models in vitro and in vivo. Isolation of the BmooMP- α -I enzyme from the crude venom of the B. moojeni snake was performed using DEAE Sephacel, Sephadex G-75 and Benzamidine-Sepharose chromatography columns. Two-dimensional (2D) electrophoresis showed degree of purity, molecular mass (Mr) and isoelectric point (pI) in non-reducing conditions only one protein spot can be evidenced (~ 23.0 kDa; pI 6.82). The levels of TNF determined by the ELISA method were significantly reduced in the presence of the enzyme BmooMP- α -I, suggesting that it exerts a proteolytic action on TNF, which was confirmed by the disappearance of this cytokine among the profile of protein bands in SDS- PAGE and Western Blotting. The macrophages assayed with PRR agonists, demonstrated a reduction in levels of TNF secreted by macrophages after their treatment with the enzyme BmooMP- α -I. In vivo studies (septic shock test and DSS-induced colitis) have also shown that BmooMP- α -I is able to reduce levels of circulating TNF and ameliorate other aspects of the inflammatory bowel disease. In conclusion, BmooMP- α -I metalloprotease presents an anti-inflammatory profile of immune response, resulting from its direct action on the proinflammatory cytokine TNF.

Keywords: *Bothrops moojeni*, BmooMP- α -I, TNF

APRESENTAÇÃO

O presente trabalho refere-se à purificação de uma biomolécula, denominada BmooMP-alfa-I, uma enzima da classe P-I das metaloproteases isolada da peçonha da serpente brasileira *Bothrops moojeni* e o seu papel biológico dentro do processo de inflamação. A inflamação é uma reação de quebra á homeostase mediado por várias moléculas e células tendo como consequência os processos patológicos. Dentre estes eventos, a típica liberação de citocinas pro-inflamatórias, como por exemplo, TNF.

O fator de necrose tumoral (TNF) é uma citocina homotrimérica essencial na mediação da inflamação produzido como uma molécula transmembrana inativa e sua forma solúvel ativa resultante de sua clivagem proteolítica pela enzima TACE (Enzima Conversora do Fator de Necrose Tumoral). As interações não covalentes entre as unidades monoméricas enoveladas formam um trímero estável de TNF. Ambos as formas de TNF solúvel e transmembrana podem sinalizar via dois diferentes receptores, receptores TNFRI e TNFRIL. Para ambos os receptores, a via de sinalização ocorre por meio da ligação da molécula trimérica de TNF com o seu receptor.

O principal efeito fisiológico de TNF em condições homeostáticas é desencadear a resposta imunológica e inflamatória pelo recrutamento indireto de neutrófilos e monócitos para o local da infecção promovendo sua ativação. Em concentrações fisiológicas, TNF atua nas células endoteliais promovendo a vasodilatação e estimulando a secreção pelos leucócitos das citocinas e quimiocinas, contribuindo no combate a infecção local (VITALE, ANDRADE, RIBEIRO, 2007).

No entanto, apesar de TNF ser essencial no combate a infecções, o desequilíbrio na sua produção está ligado diversas doenças autoimunes como artrite reumatoide, doença de Crohn's, psoríase entre outras. Em alguns pacientes, a inibição da atividade de TNF pode ocorrer via o bloqueio por anticorpos ou pela fusão da proteína com os anticorpos e seus receptores resultando na supressão da atividade de TNF e em alguns casos remissão do quadro clínico da patologia. Atualmente existem cinco inibidores de TNF aprovados para o uso clínico: três anticorpos de cadeia leve (infliximab, adalimumab e golimumab), a PEGy Fragmento Fab (certolizumab pegol), e um fragmento Fab ligado ao Receptor-Fc (etanercept). Todos os inibidores de TNF bloqueiam a ligação do TNF aos seus receptores. Porém, pouco se sabe sobre o destino dos complexos TNF-anti-TNF, sua estabilidade, tamanho, taxa de depuração e captação pelas células apresentadoras de antígenos, o que pode contribuir para seu potencial imunogênico destes inibidores de TNF, além dos eventos adversos.

Nesta perspectiva, estudos de longo prazo devem ser realizados com intuito de revelar os verdadeiros efeitos do bloqueio de TNF e suas consequências para os pacientes, relacionando os

riscos de co-morbidade, genética individual e a produção de antiglobulinas (Anticorpos produzidos contra os anticorpos monoclonais anti- TNF).

Entre as soluções alternativas desenvolvidas pela indústria farmacêutica são os chamados biofármacos, produtos farmacêuticos derivados de componentes ativos obtidos por síntese química e outros sintetizados por organismos vivos, principalmente proteínas e/ou um ácido nucléicos.

Os compostos farmacêuticos produzidos a partir da peçonha de serpentes são biofármacos de origem biológica derivados de proteínas isolados a partir da mesma, ou como moléculas análogas a estas proteínas ou até mesmo peptídeos sintetizados a partir de estrutura molecular destes compostos.

Neste sentido, a presente tese desenvolvida no Laboratório de Pesquisa em ImunoParasitologia da Universidade Federal de Uberlândia tem por objetivos principais: 1) Caracterizar bioquímica e estruturalmente a atividade proteolítica da metaloprotease BmooMP-alfa-I, isolada da peçonha de *Bothrops moojeni* sobre a citocina pró-inflamatória TNF em modelos experimentais *in vitro* e *in vivo*; 2) Determinar por meio de análise *in silico* a possível sequência de aminoácidos de TNF clivada pela enzima BmooMP-alfa-I; 3) Analisar o efeito da metaloprotease BmooMP-alfa-I e seu potencial terapêutico sobre os modelos *in vivo* de choque séptico e colite ulcerativa. Esta tese foi subdividida em 3 capítulos, conforme apresentado a seguir:

Capítulo I- Interaction between TNF and BmooMP-Alpha-I, a Zinc Metalloprotease Derived from *Bothrops moojeni* Snake Venom, Promotes Direct Proteolysis of This Cytokine: Molecular Modeling and Docking at a Glance. Artigo publicado no periódico *Toxins*, em julho de 2016, apresentando os resultados da purificação e caracterização bioquímica da atividade biológica de BmooMP-alfa-I sobre a citocina TNF e análises *in silico*;

Capítulo II- Treatment with a zinc metalloprotease purified from *Bothrops moojeni* snake venom (BmooMP-alpha-I reduces the inflammation in an experimental model of dextran sulfate sodium-induced colitis. Artigo foi aceito para publicação no periódico *Mediators of Inflammation*, apresentando os resultados do efeito de BmooMP-alfa-I sobre a colite ulcerativa induzida por DSS em camundongos;

Capítulo III- Perspectivas futuras – apresenta em linhas gerais as pesquisas a serem realizadas para elucidar com mais detalhes a interação e especificidade de clivagem de BmooMP-alfa-I sobre TNF.

Capítulo I: SILVA, M.C *et al.* 2016

Interaction between TNF and BmooMP-Alpha-I, a Zinc Metalloprotease Derived from *Bothrops moojeni* Snake Venom, Promotes Direct Proteolysis of This Cytokine: Molecular Modeling and Docking at a Glance

Maraisa Cristina Silva ¹, Tamires Lopes Silva ¹, Murilo Vieira Silva ¹, Caroline Martins Mota ¹,
Fernanda Maria Santiago ¹, Kelly Cortes Fonseca ², Fábio Oliveira ², Tiago Wilson Patriarca Mineo ¹
and José Roberto Mineo ^{1,*}

¹ Institute of Biomedical Sciences, Laboratory of Immunoparasitology “Dr. Mario Endsfeldz Camargo”, Federal University of Uberlândia, Av. Pará 1720, Uberlândia 38400-902, Brazil; maraisacris@doutorado.ufu.br (M.C.S.); tlopes_s@yahoo.com.br (T.L.S.); murilo.vieira@ufu.br (M.V.S.); carolinemartinsm@doutorado.ufu.br (C.M.M.); nandasantiago@hotmail.com (F.M.S.); tiago.mineo@ufu.br (T.W.P.M.);

² Institute of Biomedical Sciences, Laboratory of Biophysics, Federal University of Uberlândia, Av. Pará 1720, Uberlândia 38400-902, Brazil; kellyfonseca2003@yahoo.com.br (K.C.F.); foliveira@umarama.ufu.br (F.O.)

* Correspondence: jrmineo@ufu.br; Tel.: +55-34-3225-8668; Fax: +55-34-3225-8672

Academic Editor: Stephen P. Mackessy

Received: 17 December 2015; Accepted: 7 July 2016; Published: date

Abstract: Tumor necrosis factor (TNF) is a major cytokine in inflammatory processes and its deregulation plays a pivotal role in several diseases. Here, we report that a zinc metalloprotease extracted from *Bothrops moojeni* venom (BmooMP-alpha-I) inhibits TNF directly by promoting its degradation. This inhibition was demonstrated by both in vitro and in vivo assays, using known TLR ligands. These findings are supported by molecular docking results, which reveal interaction between BmooMP-alpha-I and TNF. The major cluster of interaction between BmooMP-alpha-I and TNF was confirmed by the structural alignment presenting Ligand Root Mean Square Deviation LRMS = 1.05 Å and Interactive Root Mean Square Deviation IRMS = 1.01 Å, this result being compatible with an accurate complex. Additionally, we demonstrated that the effect of this metalloprotease on TNF is independent of cell cytotoxicity and it does not affect other TLR-triggered cytokines, such as IL-12. Together, these results indicate that this zinc metalloprotease is a potential tool to be further investigated for the treatment of inflammatory disorders involving TNF deregulation.

Keywords: BmooMP-alpha-I; zinc metalloprotease; TNF; TACE

1. Introduction

TNF is a classical pro-inflammatory cytokine involved in the modulation of acute inflammatory responses and host defense mechanisms [1]. However, increased levels of this cytokine are closely associated with degenerative diseases, such as sepsis, rheumatoid arthritis, and inflammatory bowel disease, among others [2]. It is mainly produced by monocytes and secreted as a transmembrane protein (mTNF-26 kDa) and cleaved by the TNF-converting enzyme (TACE), a zinc metalloprotease, in its soluble form (sTNF-17 kDa). Both fragments are biologically active and bind as trimers to either TNF receptors, TNFR1 (also referred as TNFRSF1A, p55, or CD120a) or TNFR2 (also called TNFRSF1B, p65, or CD120b) [3,4]. Currently, monoclonal antibodies against TNF are commercially available to treat TNF-mediated pathologies. These antibodies are most frequently applied for treatment of rheumatoid arthritis, and promising results have been obtained for treatment of other inflammatory disorders [5].

Metalloproteases are enzymes characterized by presenting a catalytic zinc ion in its active site [6]. Snake venom metalloproteases (SVMPs) represent at least 30% of the toxin composition of many viperid snake venoms and they are responsible for hemorrhage through disturbances in the blood coagulation cascade of prey and snakebite victims [6]. However, certain SVMPs lack hemorrhagic activity (P-I class of SVMPs), but present other biological effects, such as inhibition of platelet aggregation, induction of apoptosis, and pro- or

anti-inflammatory activities [7–9]. SVMPs are phylogenetically most closely related to the mammalian ADAM (a disintegrin and metalloprotease) and ADAMTS (ADAM with thrombospondin type-1 motif) family of proteins and, together, they constitute the M12B clan of metalloendopeptidases [6].

The SVMPs are divided into three main classes according to their domain organization: SVMPs of the class PI contain only the metalloprotease domain in the mature protein, including the canonical zinc-binding motif HEXXHXXGXXH followed by a Met-turn motif. The class PII is comprised of enzymes containing a disintegrin domain following the metalloprotease domain. Class PIII SVMPs contain the metalloprotease domain, the disintegrin-like (Dis-like) domain and a cysteine-rich domain (Cys-rich). Post-translational processing of precursors of some PIII metalloproteinases results in the release of the Dis-like and Cys-rich domains (DC fragment) [10,11]. Additional heterogeneity of these enzymes arises from the occurrence of PII and PIII SVMP dimers, and there are PIII SVMPs that contain an additional subunit constituted by a C-type lectin-like protein, linked to the main proteinase chain by disulfide bonds [7,10,11].

BmooMP-alpha-I isolated from *B. moojeni* snake venom is a fibrin(ogen)olytic and non-hemorrhagic zinc metalloprotease of the class PI SVMPs with a molecular mass of 24.5 kDa [12,13]. This enzyme exerts its biological activity by cleaving first the A-alpha-chain of fibrinogen, followed by its B-beta-chain, but with no effects on the gamma-chain. Also, it lacks hemorrhagic and thrombin-like activities [12].

Previous study of the crystal structure of BmooMP-alpha-I showed that the enzyme presents a catalytic zinc ion displaying an unusual octahedral coordination, which includes three canonical histidines [13]. From this structural study, as well as from comparative sequence analysis, it was concluded that the motif comprising amino acid segments 153–164 and 167–176 adjacent to the methionine-turn is a relevant feature that differentiates non-hemorrhagic and hemorrhagic class P-I SVMPs, and could directly be involved in the development of the hemorrhagic activity [13].

Studies of BmooMP-alpha-I to date have focused only on its fibrin(ogen)olytic and non-hemorrhagic activity. The major aim of the present study was to investigate whether this metalloprotease could modulate TNF inflammatory properties, considering that the precursor form of this cytokine is targeted by TACE, another metalloprotease from the same class (zinc-dependent metalloendopeptidases).

2. Results and Discussion

Venoms secreted by snakes constitute a complex mixture of molecules with various biological activities directed to different targets [14]. This is an evolutive adaptation and well-integrated system of proteins and organic constituents, used as a defense by the snakes, as it leads to the immobilization, death, and digestion of the preys [15]. The most evident activity of venoms produced by *Bothrops* snakes is proteolysis, which is responsible for the main clinical manifestations of bothropic accidents [16].

In the present study BmooMP-alpha-I was isolated from crude venom by using combined chromatographic protocols. Ion exchange chromatography on DEAE-Sephacel column resulted in the separation of five protein fractions, (peaks E1–E5) (Figure 1A). Fraction E2, which showed substantial proteolytic activity towards azocasein and fibrinogen [12], was chosen for additional procedure, based on chromatography in a Sephadex G-75 column. These procedures resulted in three peaks named E2G1, E2G2, and E2G3 (Figure 1B). The peak E2G2 showed major protein concentration and proteolytic activity and was submitted for further fractionation based on a Benzamidine-Sepharose column, resulting in two new fractions, named B1–B2. The peak B1 corresponded to the metalloprotease BmooMP-alpha-I (Figure 1C). BmooMP-alpha-I represented a quantity of 8.71% of the whole crude venom of *B. moojeni*, a significant amount if compared with other fibrin(ogen)olytic enzymes isolated from similar preparations [12,15–17].

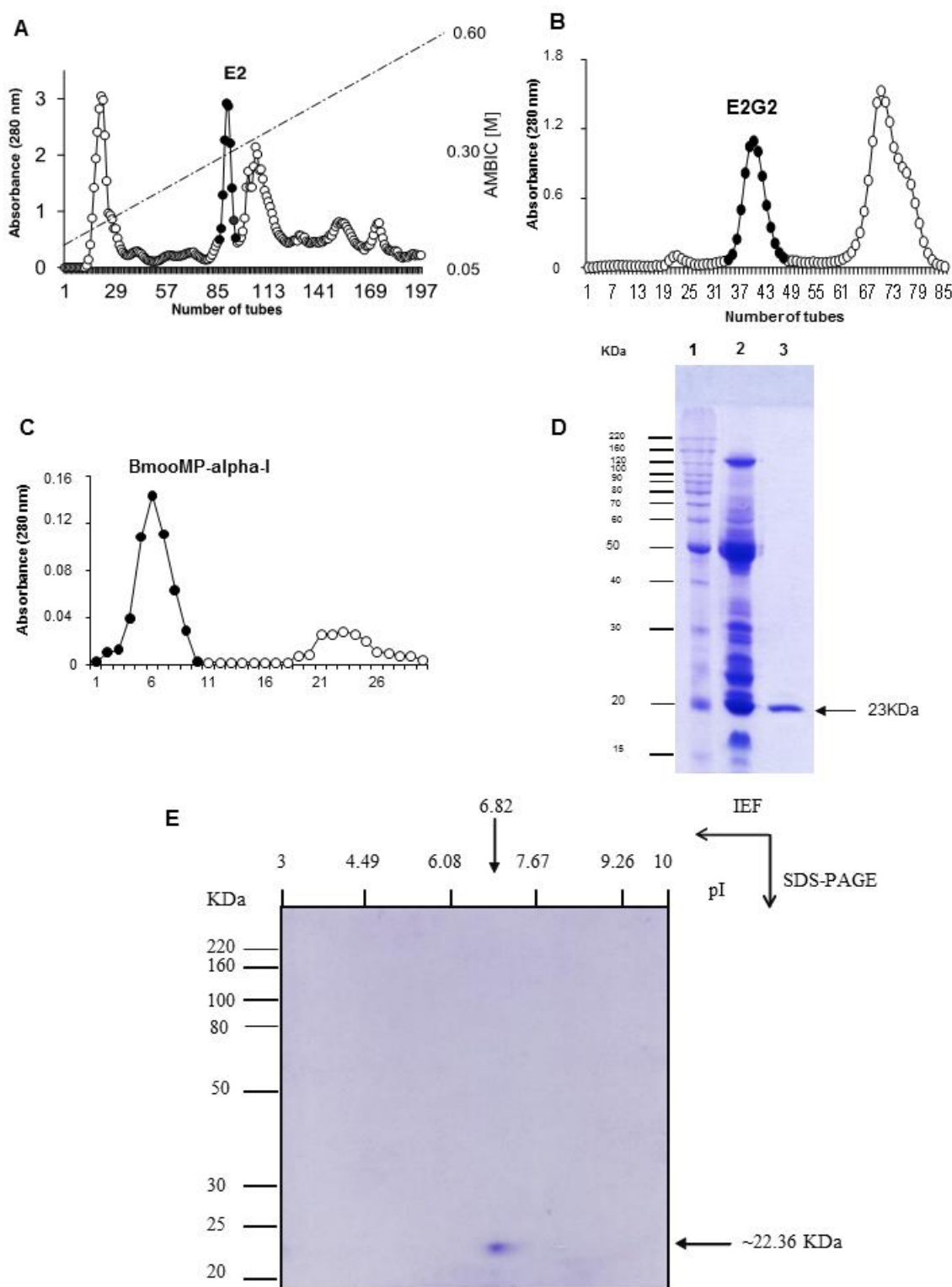


Figure 1. Purification of BmooMP-alpha-I from *Bothrops moojeni* snake venom. **(A)** Separation on DEAE-Sephacel: crude venom (400 mg) was applied on the column (1.7×15 cm) and elution was carried out at 20 mL/h flow rate with ammonium bicarbonate (AMBIC) gradient buffer, pH 7.8, from 50 mM to 0.60 M; **(B)** Separation on Sephadex G-75: the active fraction (E2) was applied on the column (1.0×100 cm) and elution with 50 mM ammonium bicarbonate buffer at pH 7.8 was achieved at a flow rate of 20 mL/h; **(C)** Separation on Benzamidine Sepharose the fraction concentrate (E2G2) was applied on the column (20×15 cm) and elution was carried out at 40 mL/h flow rate with 50 mM glycine at pH 3.0. Pooled fractions are indicated by the closed circle; **(D)** SDS-PAGE in 12% (w/v). Lanes: 1—standard proteins; 2—non-reduced crude venom B.

moojeni; 3–non-reduced BmooMP- α -I; (E) 2D electrophoresis of BmooMP- α -I solubilized in isoelectric focalization (IEF) solution were resolved by IEF capillary gel and then in 12% SDS-PAGE.

Next, 1D and 2D electrophoretic analysis was carried out of the B1 fraction under non-reducing conditions. 1D SDS-PAGE confirmed BmooMP- α -I as a monomer, with apparent molecular mass of 23 kDa (Figure 1D). The BmooMP- α -I fraction was further analyzed by 2D SDS-PAGE and the apparent molecular mass was calculated as 22.36 kDa, with pI ~6.82 (Figure 1E).

The effect of BmooMP- α -I fraction was assessed for TNF production by BMDMs stimulated with known TLR ligands. Treatment of BMDMs with BmooMP- α -I reduced significantly the TNF detection in LPS-primed macrophages for all enzyme concentrations that were tested (Figure 2A). In contrast, no significant alteration was observed in the levels of IL-12 after treatment with the same concentrations of the metalloprotease (Figure 2B). The priming of BMDMs with TLR2/TLR6 agonist FSL-1 induced strong production of TNF, which could be inhibited by the BmooMP- α -I, when tested in concentrations of 12 and 6 μ g/mL (Figure 2C). BmooMP- α -I was also not able to alter IL-12 production (Figure 2D). Additionally, we observed that this induced effect is independent of cell cytotoxicity, as determined by MTT cell viability assay using macrophages treated with agonists and/or BmooMP- α -I (Figure S1).

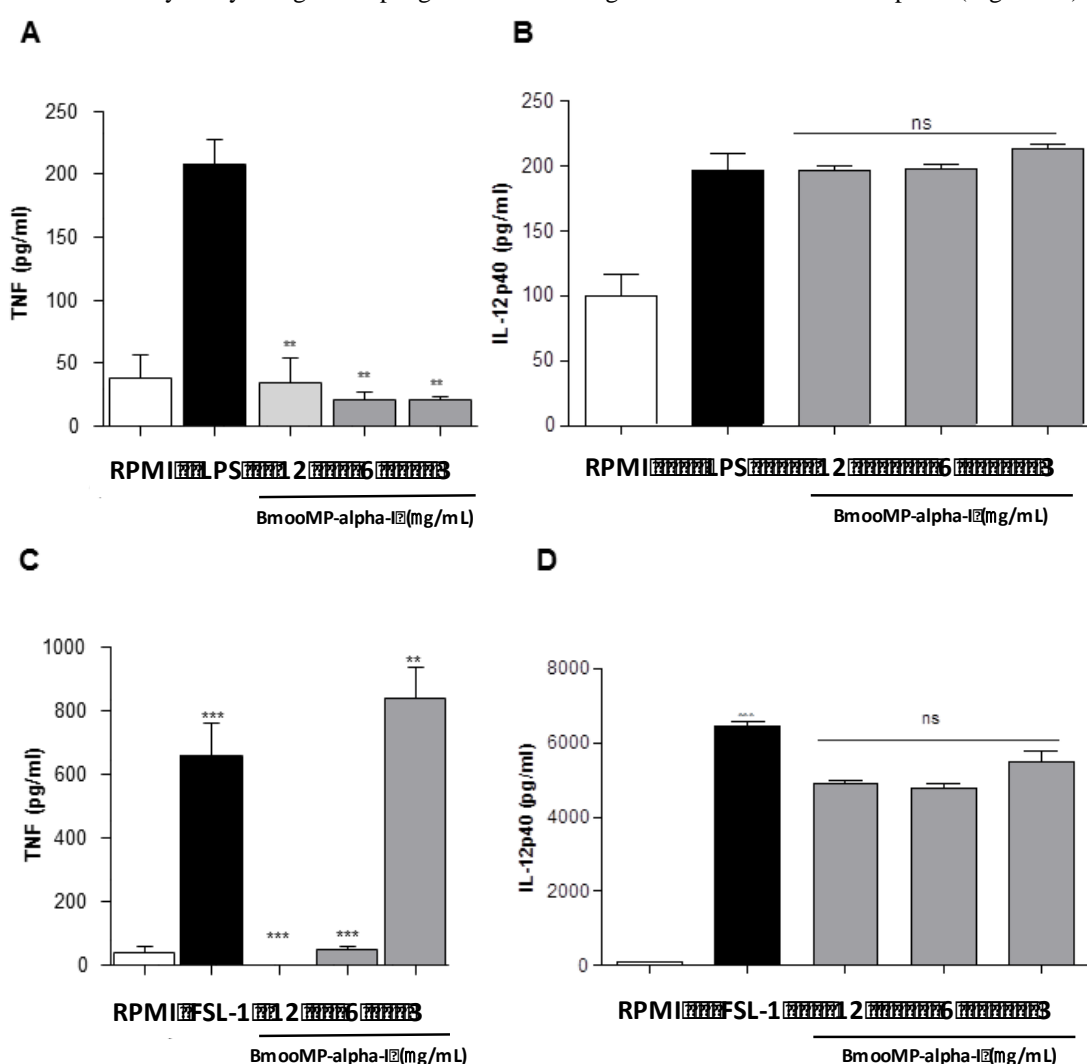


Figure 2. In vitro model for assessment of TNF production. (A) Levels of TNF determined after preincubation with LPS and treated BmooMP- α -I; (B) Levels of IL-12 p40 determined after preincubation with LPS and treated BmooMP- α -I; (C) Levels of TNF determined after preincubation with FSL-1 and treated BmooMP- α -I; (D) Levels of IL-12 p40 determined after preincubation with LPS and treated BmooMP- α -I. Macrophages were cultured in 96-well plates and after 24 h they were activated with Toll-like receptor (TLR) agonists: LPS (1 μ g/mL); FSL-1 (1 μ g/mL) or maintained with RPMI medium (control) at 37

°C and 5% CO₂. Cells were then treated with BmooMP-alpha-I (12 to 3.0 µg/mL) or maintained with RPMI medium (control) for additional 24 h at 37 °C and 5% CO₂. Levels of TNF and IL-12 were determined by ELISA kit according to the manufacturer's instructions. Results are expressed as mean ± SD and compared to untreated controls by using Two-way Anova and Bonferroni multiple comparison post-test. ** $p < 0.01$ and *** $p < 0.001$; ns: no significant in relation to controls (RPMI medium).

To further confirm the inhibitory effect of the BmooMP-alpha-I metalloprotease on TNF, we examined the effect of this enzyme in a model of LPS-induced sepsis in mice, as it was already known that death caused by septic shock is crucially dependent on TNF production [18]. It was found that the serum levels of TNF were reduced by nearly 50% in animals pre-treated with BmooMP-alpha-I, when compared with mice inoculated with PBS only (Figure 3). LPS is a major structural component of Gram-negative bacteria cell walls and it is able to induce the systemic inflammation observed in septic shock by interacting with TLR4. Upon activation of TLR4, a sequence of signal transduction events occurs, leading to the nuclear translocation of NF-κB transcription factor, which results in transcription of various inflammatory cytokines, such as TNF, IL-1-beta, and IL-12p70. It has been described that these cytokines are responsible for the systemic inflammatory response observed during septic shock [19]. Thus, strategies to decrease the TNF levels could be beneficial to control several pro-inflammatory pathologies, as the blockage of this cytokine improves the prognosis of these diseases [20].

In order to verify whether TNF was directly cleaved by BmooMP-alpha-I, additional experiments were performed. First, the effect of this metalloprotease was determined on degradation of TNF or IL-12 by ELISA. Levels of TNF were determined under different conditions, as TNF and IL-12 standard cytokines or antibodies against them (capture antibodies) were incubated with the following preparations: pure protein (BmooMP-alpha-I); BmooMP-alpha-I inactivated with NA₂EDTA (BmooMP-alpha-I(i)). It was observed that the levels of TNF decreased by 53.4% after incubation with the pure metalloprotease. In addition, the level of TNF was restored by 80% in the presence of NA₂EDTA (Figure 4A). In contrast, no significant alterations were observed in IL-12 levels submitted to the same experimental conditions (Figure 4B). As controls, ELISA plates pre-sensitized with capture antibodies were previously incubated with pure protein (BmooMP-alpha-I), or BmooMP-alpha-I inactivated with NA₂EDTA (BmooMP-alpha-I(i)). As demonstrated in Figure 4C,D, no significant alteration on the levels of TNF was observed. As shown in Figure 4C, the capture antibodies protect TNF from degradation by possibly masking the proteolytic sites in TNF, corroborating with the direct effect of BmooMP-alpha on TNF. Additional evidence was observed on the fact that the amount of TNF was not reduced in the presence of NA₂EDTA, a chelating agent used to remove bivalent ions, which completely eliminates the biological activity of SVMPs [21]. Furthermore, the polyclonal antibody anti-BmooMP-alpha-I probably binds to different domains from the catalytic domain of the enzyme responsible for catalyzing the proteolysis of TNF [22,23].

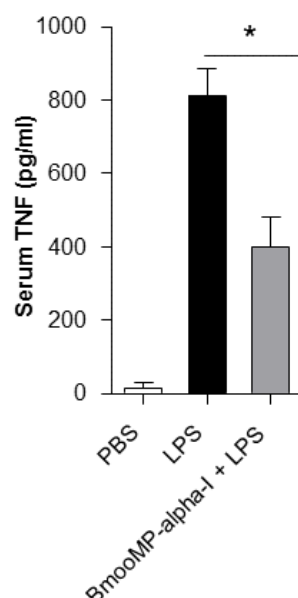


Figure 3. In vivo model for assessment of TNF production. Mice were divided in groups ($n = 10$ per group) treated with the following conditions: PBS (control); PBS plus 100 μg of LPS (PBS + LPS); or BmoMP-alpha-I (50 μg) plus 100 μg of LPS (BmoMP-alpha-I + LPS). All animals received a final volume of 1 mL into their peritoneal cavity; the pretreatment was realized over 1 h and stimulated with LPS for 90 min. Serum TNF levels were measured by ELISA. The results are expressed as mean \pm SD in triplicate for each experimental condition, and compared by using One-Way Anova and Tukey's Multiple Comparison Test. * $p < 0.05$ in relation to the group of control (mice that received injection with PBS, only).

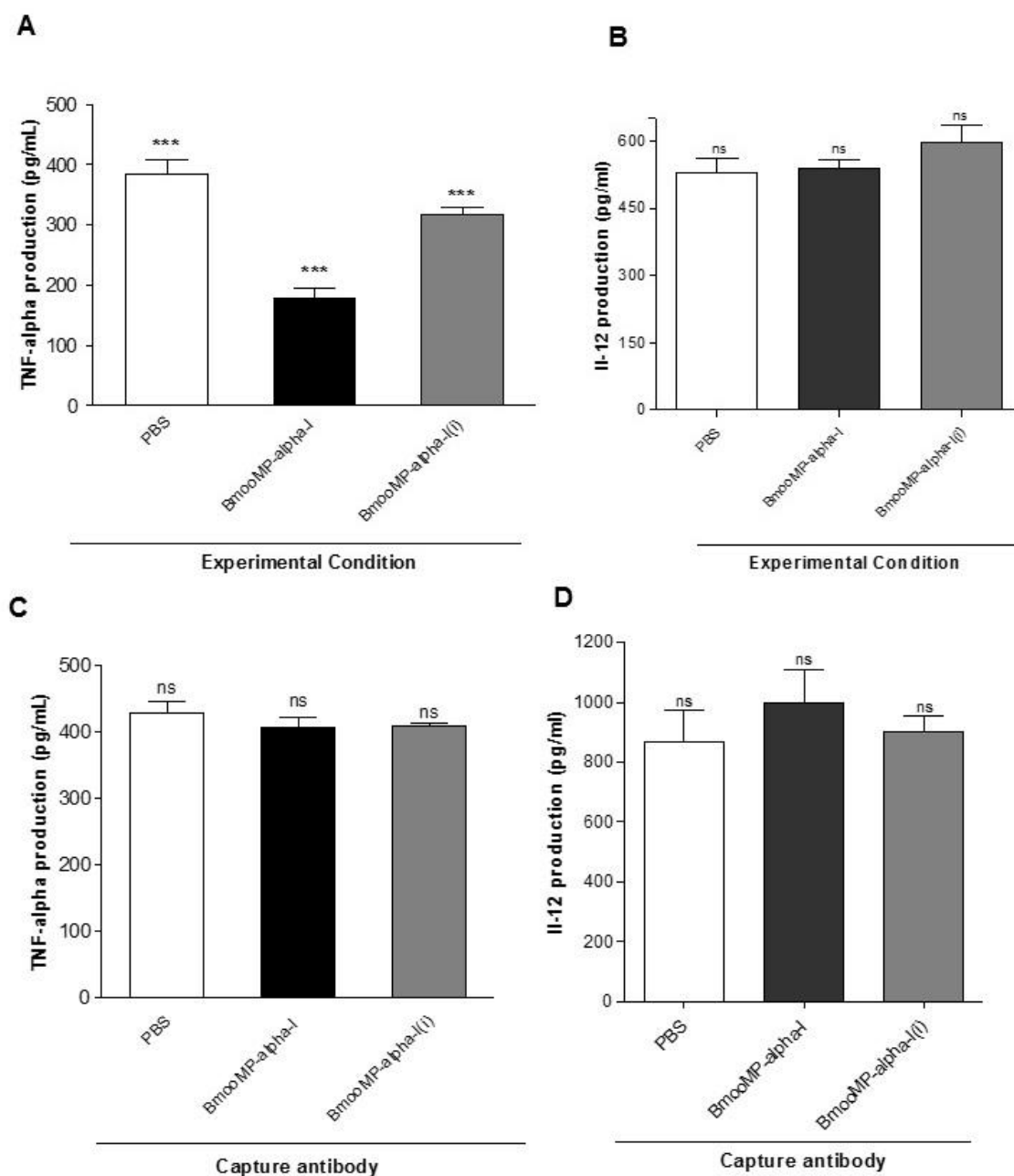


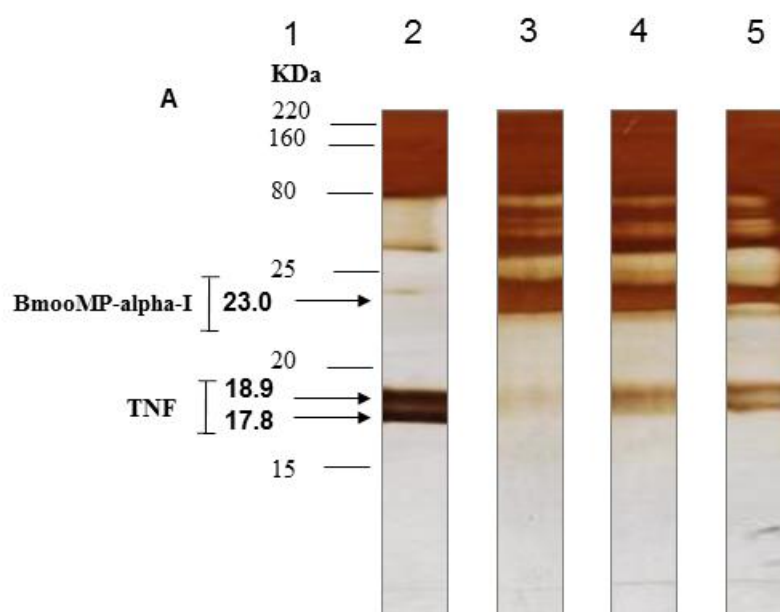
Figure 4. Inhibitory effect of BmoMP-alpha-I on the TNF detection. (A) Determination of TNF levels; (B) Determination of IL-12 levels. The cytokines were detected after preincubation of capture antibody with 12 $\mu\text{g/mL}$ BmoMP-alpha-I or 10 mM EDTA treated BmoMP-alpha-I (BmoMP-alpha-I(i)) for 45 min at 37 $^{\circ}\text{C}$; (C) Determination of TNF levels (D) Determination of IL-12 levels. Now, the cytokines were detected after preincubation of recombinant TNF or IL-12 with 12 $\mu\text{g/mL}$ BmoMP-alpha-I or 10 mM EDTA treated BmoMP-alpha-I (BmoMP-alpha-I(i)) for 45 min at 37 $^{\circ}\text{C}$. Negative control was incubated only with sterile PBS. Levels of mouse recombinant TNF were quantified by ELISA kit according to the manufacturer's instructions (DY 410-R & D Systems). Bars represent means \pm SD out of five analyses for each experimental

condition. Comparisons were carried out by using One-Way Anova and Dunnett's Multiple Comparison Test.

*** $p < 0.001$; ns: not significant in relation to the negative controls.

To confirm the proteolysis of TNF by metalloprotease BmooMP- α -I and to assess whether this effect could present a dose-dependent fashion, additional 1D SDS-PAGE and Western blotting experiments were carried out. The 1D SDS-PAGE with silver stained gel showed that 12 $\mu\text{g/mL}$ of BmooMP- α -I was active against TNF and caused a degradation of this substrate, which could be evidenced by the fading of its chains, as demonstrated by the electrophoretic profile of the reaction (Figure 5A). The concentrations of 6 $\mu\text{g/mL}$ and 3 $\mu\text{g/mL}$ of BmooMP- α -I impaired the proteolytic activity towards TNF in a dose-dependent fashion, although the effect was still present at the lower concentration (Figure 5A,B). These results obtained by Western blotting demonstrated that BmooMP- α -I is able to impair TNF levels to a point that was not recognized by its specific monoclonal antibody (Figure 5C), suggesting that the biological effect imposed by the metalloprotease induced the loss of the TNF tridimensional structure. These findings are in agreement with previous results in the literature concerning a recombinant fibrinogenase rF II, designed from a metalloprotease of *Agkistrodon acutus* snake, which showed a protective role in sepsis by promoting proteolysis of fibrin and TNF, accompanied by a decrease of the plasmatic concentration of this cytokine [24,25]. The same recombinant fibrinogenase rF II showed a protective role in a model of acute severe pancreatitis induced by sodium taurocolate that was dependent of TNF proteolysis [26].

To explore the mechanism of the protein-protein interaction, docking analyses of BmooMP- α -I protein (3GBO) and TNF (2TNF) were performed using the available protein structures (PDB), followed by structural alignment in the Swiss PDB Viewer. The major cluster of interaction between BmooMP- α -I and TNF was confirmed by the structural alignment that presented LRMS = 1.05 Å and IRMS = 1.01 Å (Figure S2). This result is compatible with a realistic complex, once the docking possesses high accuracy had been demonstrated, when (LRMS \leq 1.0 Å or IRMS \leq 1.0 Å), intermediate accuracy (LRMS \leq 5.0 Å or IRMS \leq 2.0 Å), tolerable accuracy (LRMS \leq 10.0 Å or IRMS \leq 4.0 Å), and unrealistic (LRMS $>$ 10.0 Å and IRMS $>$ 4.0 Å) [27–29]. The ZDOCK benchmark 3 docking validation, which considers conformational changes occurring between unbound and bound state of the ligand, also presented similar classification to that utilized in the present study, defining the interaction as uncomplicated (C_{α} -I_rmsd $<$ 1.5 Å), intermediate ($1.5 \text{ Å} < C_{\alpha}$ -I_rmsd \leq 2.2 Å), and hard (C_{α} -I_rmsd $>$ 2.2 Å) [28–30]. Next, we assessed the possible binding cavities and the hydrogen bonds using Swiss Pdb Viewer. It was found that the residues Arg28, His32, Glu33, Val35, Asn36, Ser37, Met38, Gly40, Arg43, Ala49, Asn131, Leu132, Gln133, Glu135, Val136, and Val171 from metalloprotease and Gln31, Arg32, Asn39, Asp42, Leu48, Asp53, Ser86, Tyr87, Glu89, Val91, and Glu 127 from TNF constitute the interactive site of the complex. Additionally, we observed that one of the possible binding cavities interacted with TNF (Figure 6).



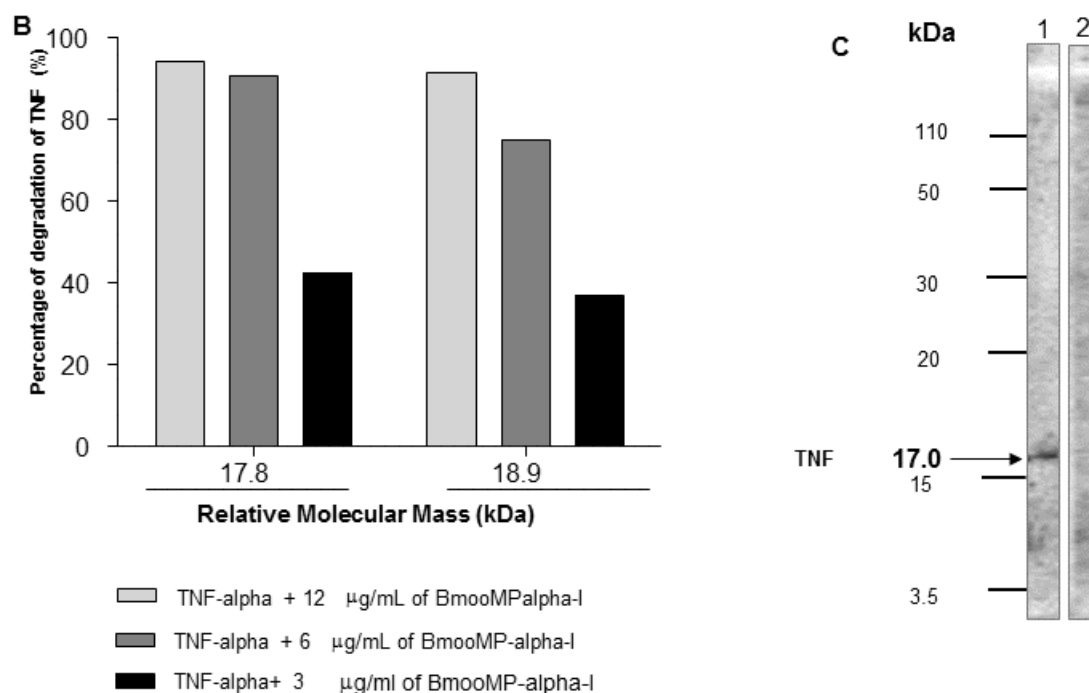


Figure 5. Direct proteolytic effect of BmooMP-alpha-I on TNF cytokine. (A) Silver stained 18% SDS-PAGE. Lanes: 1-Molecular weight standard proteins; 2-Mouse recombinant TNF without incubation with BmooMP-alpha-I enzyme (control); 3-4-Mouse recombinant TNF incubated with 12; 6; or 3 μ g/mL of BmooMP-alpha-I, respectively, for 45 min at 37 °C; (B) Percentage of TNF degradation by BmooMP-alpha-I (12; 6; and 3 μ g/mL), determined by band intensity of the reaction products estimated by Kodak 1D image software in relation to negative control versus relative molecular mass of TNF; (C) Western blot of TNF protein treated with BmooMP-alpha-I. Immunoreactive bands were developed with ECL (Electron Chemiluminescent) Western substrate and visualized with an enhanced chemiluminescence system. Lanes: 1-Mouse recombinant TNF incubated with PBS (control); 2-Mouse recombinant TNF incubated with 24 μ g/mL of BmooMP-alpha-I for 45 min at 37 °C.

In order to evaluate the stability of the potential interactions, an electrostatic analysis was carried out. The interaction between the BmooMP-alpha-I and TNF complex occurs among the following residues, respectively: Glu33-Arg32, Val171-Gln31; Ala49-Asn39; Arg28-Glu89, Arg43-Asp53; Arg43-Glu127; Arg43-Asp53; Arg43-Glu127; Val35-Asn39; Ala49-Asn39; Gln133-Gln31; Gly40-Asp42; His32-Tyr87; His32-Val91; Tyr42-Asn39; Ala49-Ser86; Val35-Tyr87 (Figure 7A,B, Figure S3A–D and Figure S5). This analysis also demonstrated several hydrogen bonds that are important for stabilization of the complex and in promoting the hydrophobic interactions, while being considered the main mechanism of action of metalloproteinases interaction, also indicating a consistent interaction between TNF and BmooMP-alpha-I [31,32]. In addition, it was possible to identify that chains A and C of TNF interact with BmooMP-alpha-I (Figure S2B), and this piece of information was further confirmed by the electrostatic potential analysis (Figure S5).

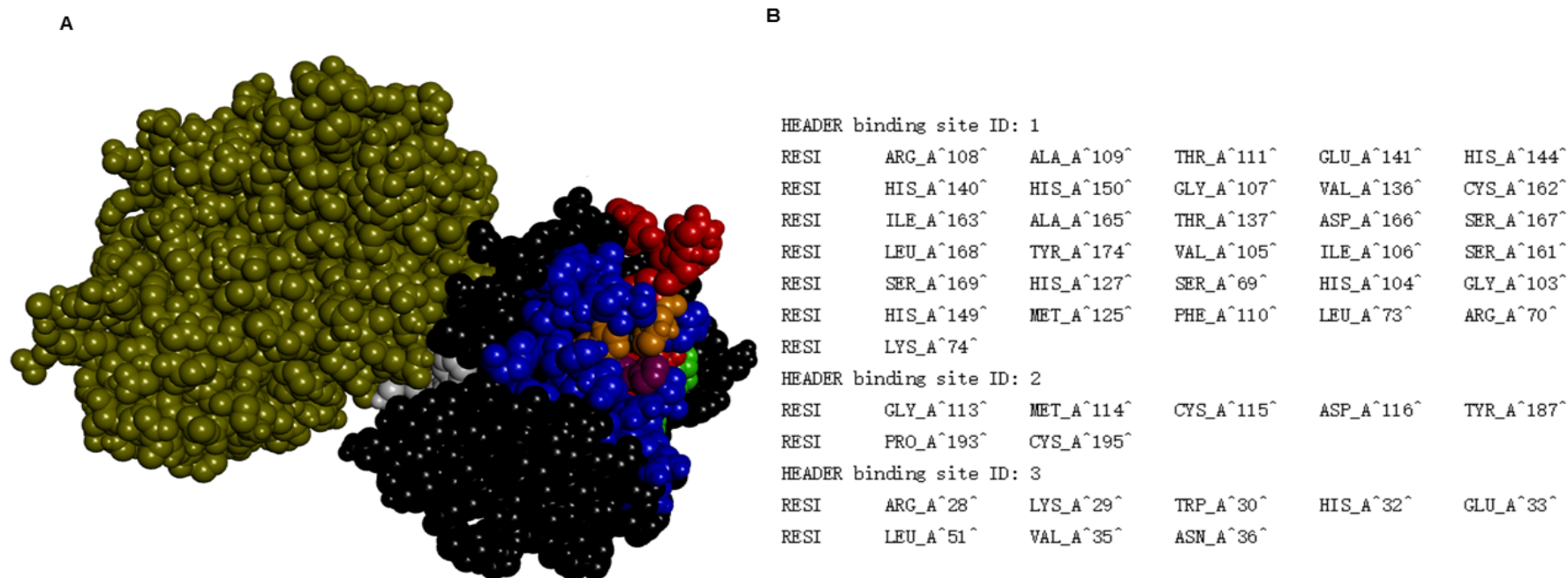


Figure 6. MetaPocket 2.0 Analysis. **(A)** 3D view of the binding cavities in the complex formed between the metalloprotease and TNF. In blue is the binding cavity 1. In green is the binding cavity 2. In white is the binding cavity 3. In purple is the conserved histidine domains. In red is the active site containing the conserved catalytic consense sequence HEXXHXXGXXH; **(B)** Table containing the amino acids sequence of each binding cavity.

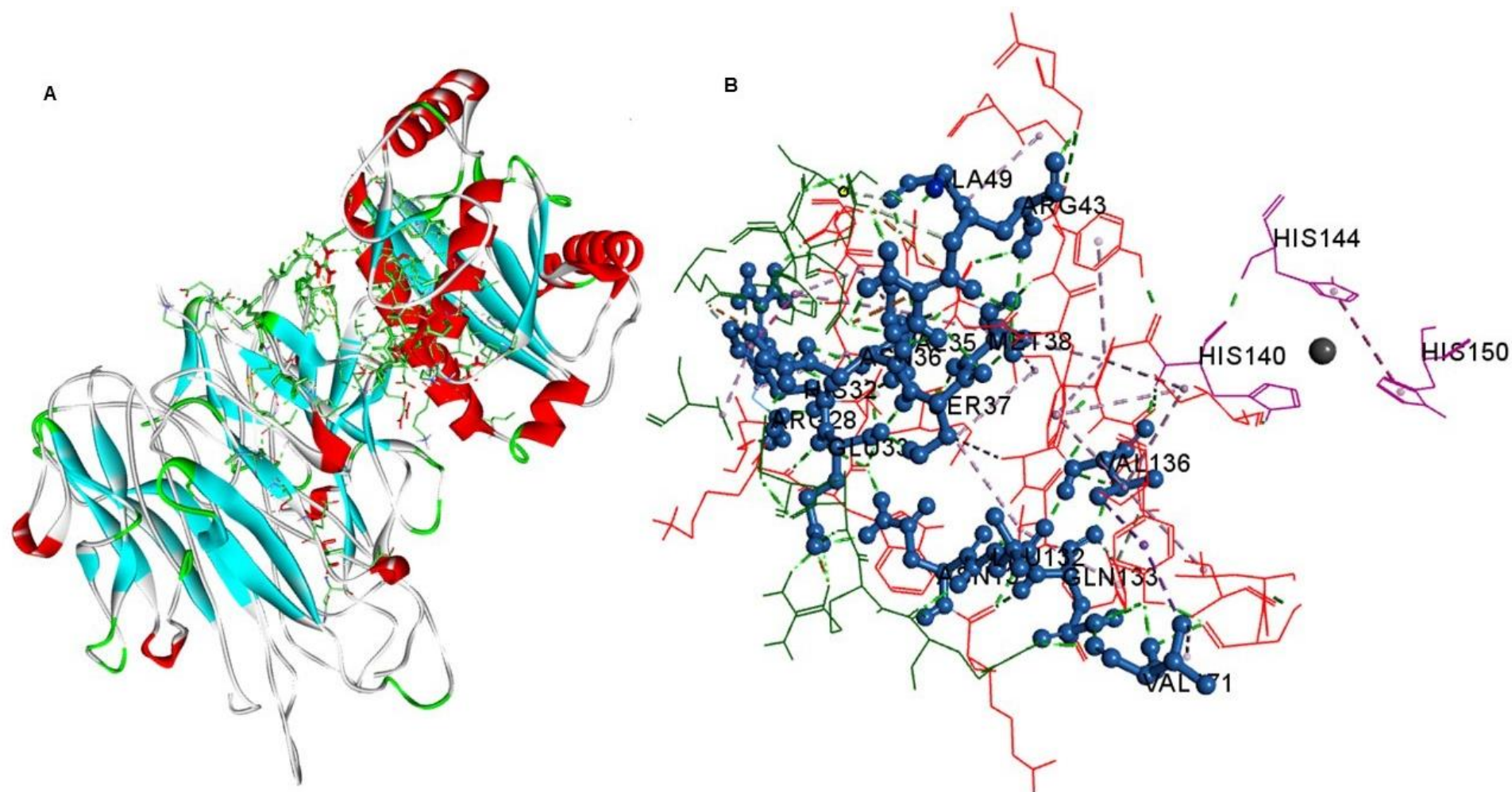


Figure 7. Analysis of the interaction of molecular complexes by Discovery Studio 3.5.0. (A) Interaction between the complex residues of 3GBO—2 TNF; (B) Demonstration of interacting residues in zoom out view. BmooMP-alpha-I is represented in red, and TNF recombinant murine in green. In purple the Zinc binding site is demonstrated.

The Ramachandran plot and alanine scanning analysis were used to validate the structure of complexes formed by protein interactions. The analysis of the complex in PDB sum generated a Ramachandran plot, where the majority of amino acids residues ($n = 98\%$) were located in allowed regions (Figure 8A). Additionally, G -factor value (0.43) was determined, which is consistent with a favorable model of interaction (G -factor > -0.5) (Figure 8B). Concerning the alanine scanning analyses, the following interacting residues were demonstrated: Arg28, Glu33, His32, Val35, Asn36, Arg43, Val136, Val171 in the metalloprotease and Gln31, Arg32, Asn39, Asp53, Ser86, Tyr87, Glu89, Val91, and Glu127 in TNF. As shown in Figure S4, these residues were considered important for upholding the complex. Therefore, it was found that the following residues are determinant for maintenance of the complex interaction between BmooMP- α -I and TNF, respectively: Glu33-Arg32; Val171-Gln31; Arg28-Glu89; Arg43-Asp53; Arg43-Glu127; Arg43-Asp53; Arg43-Glu127; His32-Tyr87; His32-Val91; Ala49-Ser86; and Val35-Tyr87. Indeed, alanine scanning is a powerful method to detect important interactions in protein-protein interfaces, as this detection occurs mainly by the measurement of the effect in the amino acid side-chain change in the C β carbon atom on the complex affinity [33,34]. Additionally, individual substitutions of several amino acids with alanine could generate a map that indicates which interactions are critical or not for maintenance of interactive complex. Moreover, alanine scanning is an important tool for identification of hotspot residues in protein-protein interfaces that is essential for complex maintenance [34,35].

The platform CLUSPRO has been generally used for docking analysis, as in actin-actin interaction [36]. This docking application was successfully used in the present study for assess the interaction prediction between BmooMP- α -I and TNF molecules. It was observed that the metalloprotease BmooMP- α -I interacts with the TNF through the amino acids Arg28, Glu33, His32, Val35, Asn36, Arg43, and Val171. Previous study demonstrated that this zinc metalloprotease (BmooMP- α -I) possesses an active site located in the upper domain (about 150 N -terminal residues) and lower domain (about 50 C -terminal residues), which is consistent with other metzincins, such as adamalysin-II [13]. This active site allows the binding to a variety of residues for different sites located in this protein. In addition, the active site is divided into three major subsites (S2, S1, and S'1 subsites) that can confer certain specificity to BmooMP- α -I [36]. In this context, the S1 subsite, which is composed by Ile106, Val136, His140, and Leu168, and the main-chain of residues forming the Met-turn, can interact with large, hydrophobic, neutral, side chains such as Leu, Qln, and Phe [37]. It is important to note that Gln133 interacts with Val 136 which is part of the cleavage subsite S1 of metalloprotease (Figure 7E), corroborating with our hypothesis that TNF is cleaved by this metalloprotease.

Studies of homology among sequences cleaved by metalloproteases utilizing bioinformatics have been developed once the classes of proteases possess homology on their preferential cleavage sites. For instance, a study pointed out that A and PA-BJ metalloproteases from *Bothropos jararaca* possess propensity for the amino acid arginine in the position 1, although a difference exists in the residue preferred at position 6 and 6', conferring certain specificity for the class of metalloproteases [38]. The prediction of cleavage sites carried out by PROSPER in the present study demonstrates various points where cleavage can occur, as this metalloprotease owns proline next to the P1 of cleavage (Figure 9). It was observed that several sequences cleaved by this proteinase contain proline [37], corroborating with our results. In addition, the predicted site of cleavage is probably near to the interacting residues, which also indicates the possible cleavage of TNF by this metalloprotease. Furthermore, it is possible to consider that there is recognition of the substrate after conformation change for catalyzing the substrate [39]. In this context, such type of changes in metalloproteases from cavities distant from the active site have been described, indicating a long-range communication network [40,41]. Another important fact is that, although the snake venom metalloproteases and those metalloproteases including Adam 17 (Tumor necrosis factor- α converting enzyme) possess a high conserved domain, located in the regions between the loop connecting H4 an H5 helices, it is necessary to take into account that there are variable regions among metalloproteases. These variabilities are import for substrate recognition, because this feature makes it possible to turn these regions in the substrate-binding pocket wall, as has already been described in the literature [41–43]. It is also necessary to consider that the methionine-turns are as important as the zinc catalytic domain for the metalloproteinase activity [40]. Thus, BmooMP- α -I may recognize Gln31, Arg32, Asn39, Asp53, Ser86, Tyr87, Glu89, Val91, and Glu127 in TNF and might cleave anteriorly and posteriorly the sequence QLVVPADG, considering that this sequence possesses a proline, which is an important residue recognized by the metalloprotease BmooMP- α -I.

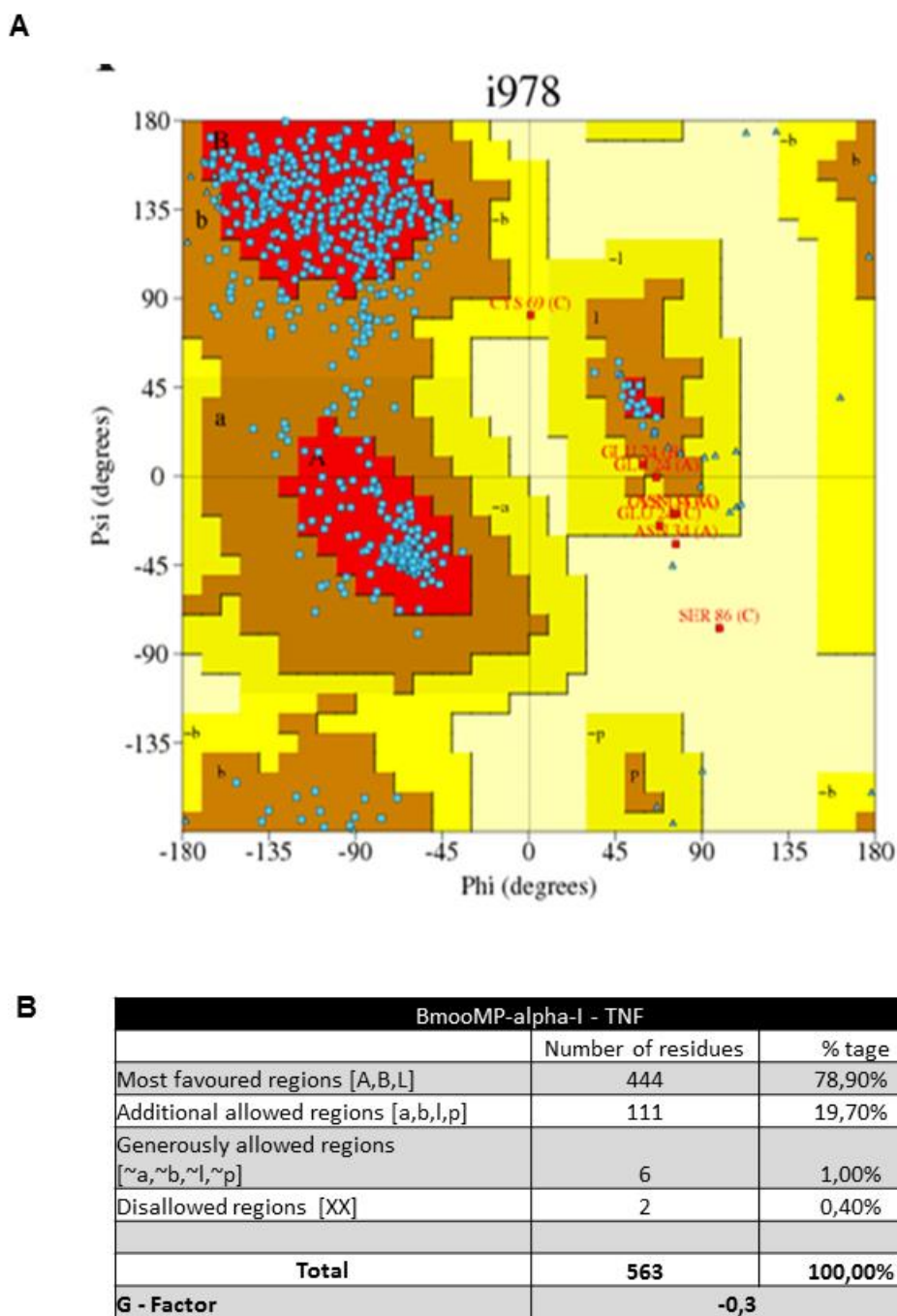


Figure 8. Ramachandran plot: **(A)** The graphic demonstrates the phi-psi torsion angles for all residues in the BmooP-alpha-I and TNF molecular complex. The coloring/shading on the plot represents the allowed phi-psi backbone conformational regions, where the darkest areas (in red) correspond to the most favorable combinations of phi-psi values; **(B)** Details of the residues number in each region of Ramachandran plot and G-score.

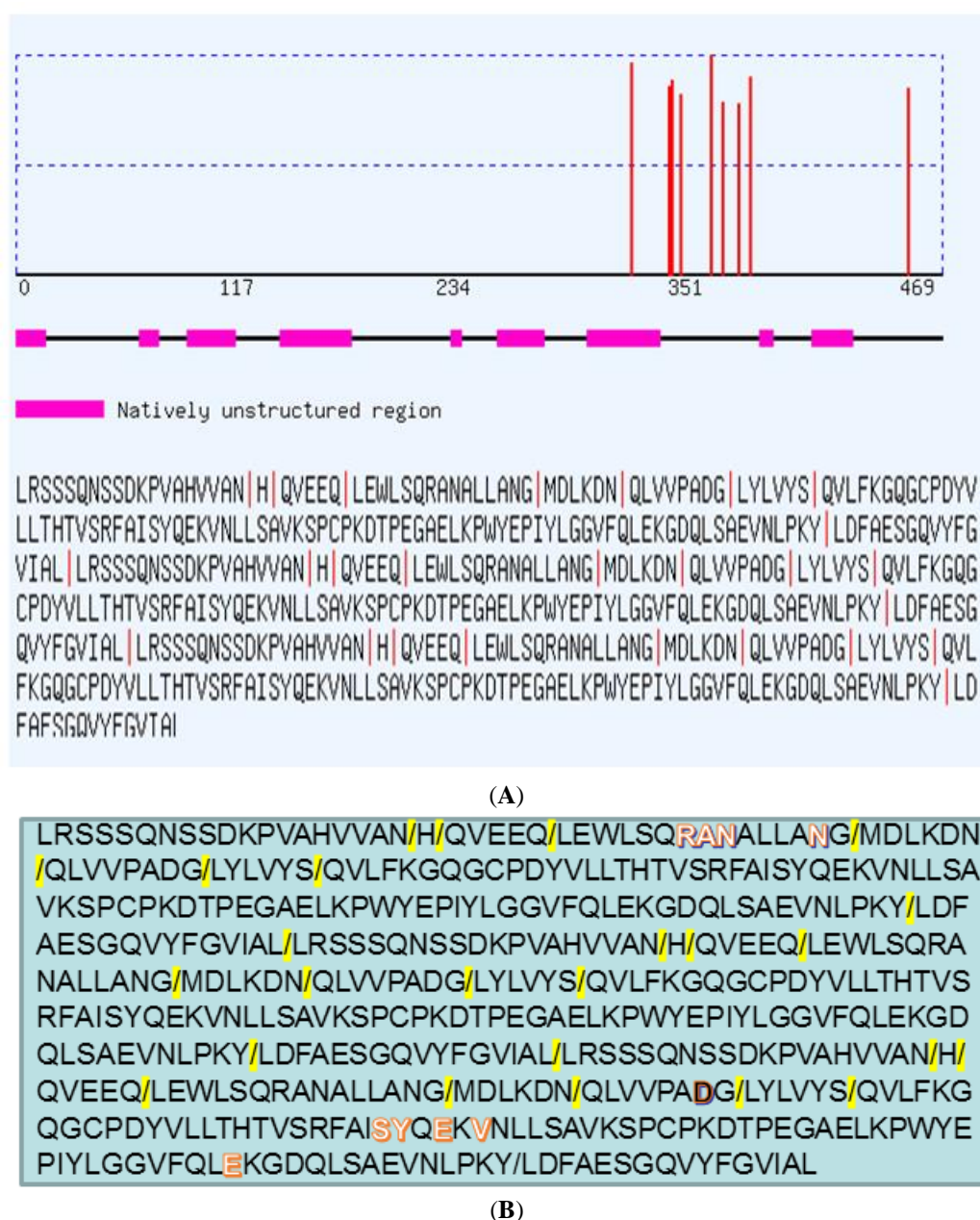


Figure 9. Analysis of the potential cleavage sites in TNF by BmooP-alpha-I metalloprotease using PROSPER by homology with other metalloproteases. (A) Predicted cleavage sites P1 in TNF that can be cleaved and the main points of cleavage by metalloproteases that are indicated as a red line in the TNF respective regions; (B) Predicted cleavage sites P1 in TNF that can be cleaved by metalloprotease in yellow and the predicted amino acids that interact with BmooMP-alpha-I, highlighted in red and white. The most reliable prediction site is highlighted in red and black.

It is important to emphasize that the metalloprotease BmooMP-alpha-I is a fibrin(ogen)olytic non-hemorrhagic SVMP that is naturally produced by *B. moojeni* which we found able to hydrolyze TNF. In the literature a high degree of homology among snake venom metalloproteases (SVMPs), metalloproteases from mammalian extracellular matrix (MMPs), and the metalloproteases from disintegrin family (ADAMs), have been described. These families of enzymes are able to degrade substrates from different sources. In this context, MMPs can cleave cytokines and chemokines, even though the existence of components from the extracellular matrix [44]. Concerning TNF, it is already known that TNF-converting enzyme (TACE) processes the precursor form of this cytokine in order to release its soluble form. Similar to the other members of the ADAM family, the structure of TACE is characterized by distinct domains that include a pro-domain, a

metalloprotease, and a disintegrin domain, followed by a cysteine-rich domain containing an epidermal growth factor (EGF)-like repeat, a transmembrane domain, and a cytoplasm tail. Considering the strong evidence that TACE is the major TNF convertase, this enzyme has attracted considerable interest as a specific therapeutic target in several inflammatory disorders, known to benefit from anti-TNF treatment, such as rheumatoid arthritis, Crohn's disease, and perhaps ulcerative colitis. Consequently, TNF has emerged as an important target for the development of the therapeutic strategies for treatment of chronic autoimmune disorders, and its inhibitors have been approved for clinical use [45]. These studies suggest that the regulation process of the proteolysis from metalloproteases is critical in providing appropriate “start” or “stop” signaling during an inflammatory response [45]. Thus, an anti-inflammatory agent may be the result of TNF light structural changes, which may hamper its biological activities [46].

In summary, the results described in the present study shed light for future investigations concerning the clinical applications of the zinc metalloprotease BmooMP- α -I, since it was demonstrated that this enzyme is able to promote significant proteolysis of TNF. The next step will be to confirm the TNF sequence that is cleaved by this metalloprotease. Therefore, future studies are necessary to determine whether this enzyme could induce protection in experimental models in vivo, particularly those involving TNF as a critical mediator of inflammatory diseases, in order to verify its potential protective role, as well as the existence of possible side effects from its therapeutic use.

3. Experimental Section

3.1. Animals

Male C57BL/6 mice (18–22 g) were housed in temperature-controlled rooms and received water and food ad libitum until enrolled in experimental conditions. These studies were approved by the Experimental Animals Committee of Universidade Federal de Uberlândia (CEUA-UFU—Protocol # 089/012, approved on 26 September 2012) in accordance with the procedures established by the University Federation for Animal Welfare.

3.2. Crude Venom and Toxin

Desiccated *B. moojeni* venom was purchased from Bioagents Serpenterium (Batatais-SP, Brazil). BmooMP- α -I was isolated and its purity and biological activity assessed as previously published [12,13], with modifications. Briefly, the purification steps included anion-exchange chromatography on DEAE-Sephacel (Sigma Chem. Co., Saint Louis, MO, USA), followed by size-exclusion chromatography on Sephadex-75 (GE Healthcare, Uppsala, Sweden) and affinity chromatography on Benzamidine-Sepharose (GE Healthcare). The purified toxin was diluted, dialyzed against 50 mM ammonium bicarbonate (pH 7.8), lyophilized, and stored at $-20\text{ }^{\circ}\text{C}$ until used. Protein concentration was determined by the Bradford method [47].

3.3. Electrophoretic Analysis

Samples of the BmooMP- α -I were boiled for 3 min in the presence of sample buffer and resolved in 1D SDS-PAGE at 12%, as previously described [12]. The slab gels were stained with Coomassie Blue R-250, 0.2% (w/v) in acetic acid:methanol:water (1:5:5, v/v) solution. The relative molecular mass of the purified enzyme was estimated by Kodak 1D image analysis software (version 3.5, Eastman Kodak Company, Rochester, NY, USA, 2001). BmooMP- α -I was also submitted to 2D electrophoresis, by taking 120 μg of samples solubilized in 125 μL of isoelectric focalization (IEF) solution (urea 8 M, bromophenol blue 0.002%, CHAPS 2%) and resolved into IEF capillary gel for 12 h, followed by 12% SDS-PAGE.

3.4. In Vitro Model for Assessment of TNF Production

To determine the effect of BmooMP- α -I in the TNF molecule, it was used an in vitro model based on bone marrow derived macrophages (BMDM) priming with known Toll-like receptor (TLR) agonists, as previously described [48]. Suspensions of 2×10^5 macrophages/well were maintained in 96-well plates in triplicates, for 24 h, in RPMI 1640 medium (ThermoFisher Scientific, Waltham, MA, USA), supplemented with 10% fetal calf serum (FCS; Cultilab, Campinas, SP, Brazil), at standard mammalian cell culture

conditions (37 °C and 5% CO₂). BMDMs were then primed with known TLR agonists (TLR4: LPS from *E. coli* K12, 1 µg/mL; TLR2/TLR6: FSL-1, 1 µg/mL; InvivoGen, San Diego, CA, USA) for 3 h. Next, BmooMP- α -I preparations were added at concentrations of 12 µg/mL, 6 µg/mL or 3 µg/mL and the plates were incubated for an additional 24 h. Supernatants were collected and stored at −80 °C until assayed for cytokine production. As negative controls, cells were incubated with medium only, while positive controls consisted of cells incubated with TLR agonists. Cell viability rates were determined by MTT assay, as previously described [49].

3.5. In Vivo Model for Assessment of TNF Production

Lipopolysaccharide (LPS) from *Escherichia coli* (serotype O111:B4; Sigma, St. Louis, IL, USA) was injected intraperitoneally (i.p.) in mice to induce acute systemic TNF, following a model for induction of endotoxic shock, as published elsewhere [18]. Briefly, C57BL/6 mice ($n = 10/\text{group}$) were pre-treated i.p. with PBS (control) or BmooMP- α -I (50 µg), 60 min prior to LPS stimulation (100 µg/mouse). Blood samples were collected from the retro-orbital plexus after 90 min of LPS challenge and serum samples were obtained by centrifugation (500 g, 10 min, 4 °C), and stored at −80 °C until assayed for cytokine measurement.

3.6. Cytokine Measurements

TNF levels were determined in supernatants from cell cultures and serum samples using a commercial ELISA kit, following the manufacturer's instructions (R & D Systems, Minneapolis, MN, USA). In addition, IL-12p40 production was also assessed in these samples, using an appropriate kit (BD, Franklin Lakes, NJ, USA). The cytokine concentrations in the samples were calculated by comparison with standard curves of the respective murine recombinant cytokine.

3.7. Inhibitory Effect of BmooMP- α -I on TNF Detection

To determine whether BmooMP- α -I was able to inhibit TNF detection, mouse recombinant protein (rTNF, 1000 pg/mL; R & D Systems) was pre-incubated with BmooMP- α -I (12 µg) or medium alone, as negative controls. Samples of BmooMP- α -I inactivated by 10 mM NA₂EDTA or BmooMP- α -I incubated for 2 h at 37 °C with specific polyclonal antibodies (pAb) were included in each assay, as additional controls. In parallel, anti-TNF antibody samples were also submitted to the same conditions, to ensure assay specificity. After incubation, the samples were submitted for detection of TNF by sandwich ELISA (ELISA kit R & D Systems).

3.8. SDS-PAGE to Assess Proteolytic Effect of BmooMP- α -I on TNF Protein

Different BmooMP- α -I masses (12 µg, 6 µg, and 3 µg) were mixed with rTNF (0.7 ng) in PBS pH 7.2 and incubated at 37 °C for 45 min. Negative controls consisted of metalloprotease masses incubated with sterile PBS only. After incubation, each sample was analyzed by 1D SDS-PAGE (18%), as previously described [50]. Gels were stained by silver nitrate staining kit (ThermoFisher Scientific, Waltham, MA USA) and band intensities were estimated by a dedicated imaging and analysis system (GE Healthcare).

3.9. Western Blotting for TNF

TNF proteolysis was further assessed by Western blotting. For this purpose, samples of rTNF (1.4 ng) were incubated with BmooMP- α -I (24 µg) or sterile PBS at 37 °C for 45 min. After incubation, the samples were electrotransferred to nitrocellulose membranes, as described [51]. Blotted membranes were blocked with 5% non-fat skim milk in PBS containing 0.05% Tween 20 (PBS-T), for 2 h at room temperature. The membranes were washed with PBS-T and probed with a monoclonal antibody directed to TNF (BD Biosciences, San Jose, CA, USA), diluted 1:250 in 1% PBS-T plus 1% skim milk, for 18 h at 4 °C. Immunoreactive bands were visualized and analyzed after assay development with chemiluminescent buffer (Promega, Madison, WI, USA), through sequential images captured by a proper imaging system (Bio-Rad, Hercules, CA, USA).

3.10. Molecular Docking

The X-ray crystallography or nuclear magnetic resonance (NMR) of the primary sequence was searched in the RCSB Protein Data Bank [52]. Both BmooMP- α -I protein (3GBO) and recombinant murine TNF (2TNF) were chosen to be analyzed. The crystals were refined using the platform ModRefiner freely available at [53]. This platform was assessed to generate algorithms that were used to build and enhance protein structures utilizing the traces of Ca established by two-step atomic-level of energy minimization. Next, molecular docking analyses were performed using the Cluspro program [54] to verify protein interaction. The BmooMP- α -I was selected as receptor and TNF as ligand, without selecting a presumed area of interaction. This docking approach utilizes Fast Fourier Transform (FFT), and it is considered an extensive assessment of simplified energy functions of the protein mutual orientations in discretized 6D space. During the procedure, the center of receptor is at the origin of the coordinated system. Meanwhile, the ligand rotates freely, being evaluated through an assumed level of discretization. Several docked structures were created, and the shape complementarity was used as scoring function. The final scoring was given according to the energy function, which was composed of the summation of the shape complementarity, electrostatic, and desolvation contributions. Additionally, the top ten structures resulting from clustering were aligned using a structural alignment by the Swiss Pdb Viewer program and ranked according to LRMS and IRMS values. The best structure, defined after alignment, was further analyzed by Swiss Pdb Viewer for H bonds identification and Discovery Studio 3.5.0 to confirm previous interaction. The protein binding cavities were identified using MetaPocket 2.0 [55]. The PDB sum platform [56] was utilized to create the Ramachandram plot. The structure was considered reliable whether G factor > -0.5 . Drugscore PPI 2.2 [57] was assessed for the alanine scanning. Finally, the platform Prosper [58] was employed for prediction of possible cleavage sites. This platform utilized homology from other known sequences to be cleaved by proteases, as a parameter to identify points of cleavage in the sequences that had already been determined.

3.11. Statistical Analysis

Statistical analysis of data concerning cytokine concentrations was performed using dedicated software (version 6.0h, GraphPad, La Jolla, CA, USA, 2015), using One-way ANOVA or Two-way ANOVA, followed by post-test comparisons. Values of $p < 0.05$ were considered significant and the results are representatives from at least three independent experiments.

Supplementary Materials: The following are available online at www.mdpi.com/2072-6651/8/7/223/s1, Figure S1: Cell viability determined by MTT assay of macrophages treated with PRR agonists and/or BmooMP- α -I. Figure S2: The docking analysis and interacting residues. Figure S3: Analysis of the BmooMP- α -I and TNF interaction by Discovery Studio 3.5.0. Figure S4: Alanine scanning analysis. Figure S5: Interaction between the residues of BmooMP- α -I and TNF.

Acknowledgments: This study was financially supported by Brazilian Research Agencies (FAPEMIG, Fundação de Amparo a Pesquisa no Estado de Minas Gerais; CNPq, Conselho Nacional de Desenvolvimento Científico e Tecnológico; CAPES, Coordenação de Aperfeiçoamento de Pessoal de Nível Superior; and FINEP/MCT (Financiadora de Estudos e Projetos do Ministério de Ciência e Tecnologia) from Brazil.

Author Contribution: M.C.S., T.L.S., T.W.P.M. and J.R.M. conceived and design the experiments; M.C.S., T.L.S., M.V.S., C.M.M., F.M.S., K.C.F. performed the experiments; F.O. contributed reagents and analysis tools; M.C.S., T.L.S., M.V.S., F.O., T.W.P.M. and J.R.M. analyzed the results; M.C.S., T.L.S., J.R.M. wrote the paper.

Conflicts of Interest: The authors declare that there are no conflicts of interest.

Abbreviations

The following abbreviations are used in this manuscript:

BmooMP- α -I: metalloprotease of class P-I from *B. moojeni* snake venom; rTNF: recombinant tumor necrosis factor; TACE: metalloprotease converter of TNF; TNF-RI, TNF-R1, TNFRSF1A, p55, p60 or CD120a: receptor I of TNF; TNF-RII TNF-R2, TNFRSF1B, p75, p80 or CD120b: receptor II of TNF; ADAM: A disintegrin and metalloproteinase; Na_2EDTA : acid ethylene-diamino-tetraacetic disodium salt; SFB: fetal calf serum; MTT: thiazolyl blue; DMF: *N,N*-dimethyl formamide; EGF: epidermal growth factor.

References

1. Osta, B.; Benedetti, G.; Miossec, P. Classical and paradoxical effects of TNF- α on bone homeostasis. *Front. Immunol.* **2014**, *5*, 48.
2. Sabio, G.; Davis, R.J. TNF and MAP kinase signalling pathways. *Semin. Immunol.* **2014**, *26*, 237–245.
3. Wallach, D. The cybernetics of TNF: Old views and newer ones. *Semin. Cell. Dev. Biol.* **2016**, *50*, 105–114.
4. Ramseyer, V.; Garvin, J.L. Tumor necrosis factor α : Regulation of renal function and blood pressure. *Am. J. Physiol. Renal. Physiol.* **2013**, *304*, 1231–1242.
5. Xixi, M.A.; Shengqian, X.U. TNF inhibitor therapy for rheumatoid arthritis. *Biomed. Rep.* **2013**, *1*, 177–184.
6. Takeda, S.; Takeya, H.; Iwanaga, S. Snake venom metalloproteinases: Structure, function and relevance to the mammalian ADAM/ADAMTS family proteins. *Biochim. Biophys. Acta* **2012**, *1824*, 164–176.
7. Paes Leme, A.F.; Sherman, N.E.; Smalley, D.M.; Sizukusa, L.O.; Oliveira, A.K.; Menezes, M.C.; Fox, J.W.; Serrano, S.M. Hemorrhagic activity of HF3, a snake venom metalloproteinase: Insights from the proteomic analysis of mouse skin and blood plasma. *J. Proteome Res.* **2012**, *11*, 279–291.
8. Markland, F.S.; Swenson, S. Snake venom metalloproteinases. *Toxicon* **2013**, *62*, 3–18.
9. Calderon, L.A.; Sobrinho, J.C.; Zaqueo, K.D.; de Moura, A.A.; Grabner, A.N.; Mazzi, M.V.; Nomizo, S.M.A.; Fernandes, C.F.C.; Zuliani, J.P.; Carvalho, B.A.; et al. Antitumoral activity of snake venom proteins: New trends in cancer therapy. *BioMed Res. Int.* **2014**, *2014*, 203639.
10. Barrett, A.J.; Rawlings, N.D.; Salvesen, G.; Woessner, J.F. Introduction. In *Handbook of Proteolytic Enzymes*; Rawlings, N.D., Salvesen, G., Eds.; Academic Press: Oxford, UK, 2013; pp. 1–4.
11. Herrera, C.; Escalante, T.; Voisin, M.B.; Rucavado, A.; Morazá, D.; Macêdo, J.K.; Calvete, J.J.; Sanz, L.; Nourshargh, S.; Gutiérrez, J.M.; et al. Tissue localization and extracellular matrix degradation by PI, PII and PIII snake venom metalloproteinases: Clues on the mechanisms of venom-induced hemorrhage. *PLoS Negl. Trop. Dis.* **2015**, *9*, e0003731.
12. Bernardes, C.P.; Santos-Filho, N.A.; Costa, T.R.; Gomes, M.S.R.; Torres, F.S.; Costa, J.O.; Borges, M.H.; Richardsons, M.; Santos, D.M.; Pimenta, A.M.C.; et al. Isolation and structural characterization of a new Fibrin(ogen)olytic metalloproteinase from *Bothrops moojeni* snake venom. *Toxicon* **2008**, *51*, 574–584.
13. Akao, P.K.; Tonoli, C.C.C.; Navarro, M.S.; Cintra, A.C.O.; Neto, J.R.; Arni, R.K.; Murakami, M.T. Structural studies of BmooMP- α -I, a non-hemorrhagic metalloprotease from *Bothrops moojeni* venom. *Toxicon* **2010**, *55*, 361–368.
14. Pithayanukul, P.; Leanpolchareanchai, J.; Sappapakorn, P. Molecular docking studies and anti-snake venom metalloproteinase activity of Thai mango seed kernel extract. *Molecules* **2009**, *14*, 3198–3213.
15. Oliveira, F.; Rodrigues, V.M.; Borges, M.H.; Soares, A.M.; Hamaguchi, A.; Giglio, J.R.; Homs-Brandeburgo, M.I. Purification and partial characterization of a new proteolytic enzyme from the venom of *Bothrops moojeni* (Caçaca). *Biochem. Mol. Biol. Int.* **1999**, *47*, 1069–1077.
16. Serrano, S.M.; Matos, M.F.; Mandelbaum, F.R.; Sampaio, C.A. Basic proteinases from *Bothrops moojeni* (Caissaca) venom-I. Isolation and activity of two serine proteinases, MSP 1 and MSP 2, on synthetic substrates and on platelet aggregation. *Toxicon* **1993**, *31*, 471–481.
17. Torres, F.S.; Rates, B.; Gomes, M.T.R.; Salas, C.E.; Pimenta, A.M.C.; Oliveira, F.; Santoro, M.M.; de Lima, M.E. Bmoo FIBMP-I: A new fibrinogenolytic metalloproteinase from *Bothrops moojeni* snake venom. *ISRN Toxicol.* **2012**, *2012*, 1–10.
18. Allie, N.; Alexopoulou, L.; Quesniaux, V.J.F.; Fick, L.; Kranidioti, K.; Kollias, G.; Ryffel, B.; Muazzam, J. Protective role of membrane tumour necrosis factor in the host's resistance to mycobacterial infection. *Immunology* **2008**, *125*, 522–534.
19. Shanmugam, A.; Rajoria, S.; George, L.A.; Mittelman, A.; Suriano, R. Synthetic Toll Like Receptor-4 (TLR-4) agonist peptides as a novel class of adjuvants. *PLoS ONE* **2012**, *7*, e30839.
20. Croft, M.; Duan, W.; Choi, H.; Eun, S.-Y.; Madireddi, S.; Mehta, A. TNF superfamily in inflammatory disease: Translating basic insights. *Trend Immunol.* **2012**, *33*, 144–152.
21. Markland, F.S. Snake venoms and the hemostatic system. *Toxicon* **1998**, *36*, 1749–1800.
22. Cardoso, R.; Homs-Brandeburgo, M.I.; Rodrigues, V.M.; Santos, W.B.; Souza, G.L.; Prudencio, C.R.; Siquieroli, A.C.; Goulart, L.R. Peptide mimicking antigenic and immunogenic epitope of neuwiedase from *Bothrops neuwiedi* snake venom. *Toxicon* **2009**, *53*, 254–261.
23. Harrison, R.A.; Wusterb, W.; Theakston, R.D.G. The conserved structure of snake venom toxins confers extensive immunological cross-reactivity to toxin-specific antibody Theakstona. *Toxicon* **2003**, *41*, 441–449.

24. Wang, R.; Cai, J.; Huang, Y.; Xu, D.; Sang, H.; Yan, G. Novel recombinant fibrinogenase of *Agkistrodon acutus* venom protects against LPS-induced DIC. *Thromb. Res.* **2009**, *123*, 919–924.
25. Wang, R.; Qiu, P.; Jiang, W.; Cai, X.; Ou, Y.; Su, X.; Cai, J.; Chen, J.; Yin, W.; Yan, G. Recombinant fibrinogenase from *Agkistrodon acutus* venom protects against sepsis via direct degradation of fibrin and TNF-alpha. *Biochem. Pharmacol.* **2008**, *76*, 620–630.
26. Luo, S.; Wang, R.; Jiang, W.; Lin, X.; Qiu, P.; Yan, G. Novel recombinant snake venom metalloprotease from *Agkistrodon acutus* protects against taurocholate-induced severe acute pancreatitis in rats. *Biochimie* **2010**, *92*, 1354–1361.
27. Huang, S.Y.; Zou, X. An iterative knowledge-based scoring function for protein-protein recognition. *Proteins* **2008**, *72*, 557–579.
28. Trellet, M.; Melquiond, A.S.J.; Bonvin, A.M. A unified conformational selection and induced fit approach to protein-peptide docking. *PLoS ONE* **2013**, *8*, e58769.
29. Krüger, D.M.; Garzón, J.I.; Chacón, P.; Gohlke, H. Drugscore PPI knowledge-based potentials used as scoring and objective function in protein-protein docking. *PLoS ONE* **2014**, *9*, e89466.
30. Hwang, H.; Pierce, B.; Mintseris, J.; Janin, J.; Weng, Z. Protein-protein docking benchmark version 3.0. *Proteins* **2008**, *73*, 705–709.
31. Apte, S.S.; Parks, W.C. Metalloproteinases: A parade of functions in matrix biology and and outlook for the future. *Matrix Biol.* **2015**, *44–46*, 1–6.
32. Verma, R.P.; Hansch, C. Matrix metalloproteinases (MMPs): Chemical-biological functions and (Q) SARs. *Bioorg. Med. Chem.* **2007**, *15*, 2223–2268.
33. Chellapandi, P. Structural, functional and therapeutic aspects of snake venom metalloproteinases. *Mini-Rev. Org. Chem.* **2014**, *11*, 28–44.
34. Anand, P.; Nagarajan, D.; Mukherjee, S.; Chandra, N. ABS-Scan: In silico alanine scanning mutagenesis for binding site residues in protein-ligand complex. *FI1000Research* **2014**, *3*, 214.
35. Morris, A.L.; MacArthur, M.W.; Hutchinson, E.G.; Thornton, J.M. Stereochemical quality of protein structure coordinates. *Proteins Struct. Funct. Bioinform.* **1992**, *12*, 345–364.
36. Ünü, A. Computational prediction of actin-actin interaction. *Mol. Biol. Rep.* **2014**, *41*, 355–364.
37. Okamoto, D.N.; Kondo, M.Y.; Oliveira, L.C.; Honorato, R.V.; Zanzporlin, L.M.; Coronado, M.A.; Araújo, M.S.; Motta, G.; Veroneze, C.L.; Andrade, S.S.; et al. P-I class metalloproteinase from *Bothrops moojeni* venom is a post-proline cleaving peptidase with kininogenase activity: Insights into substrate selectivity and kinetic behavior. *Biochim. Biophys. Acta* **2014**, *1844*, 545–552.
38. Zelanis, A.; Huesgen, P.F.; Oliveira, A.K.; Tashima, A.K.; Serrano, S.M.; Overall, C.M. Snake venom serine proteinases specificity mapping by proteomic identification of cleavage sites. *J. Proteom.* **2015**, *113*, 260–267.
39. Gunasekaran, K.; Ma, B.Y.; Nussinov, R. Is allostery an intrinsic property of all dynamic proteins? *Proteins Struct. Funct. Bioinform.* **2004**, *57*, 433–443.
40. Fox, J.W.; Serrano, S.M. Structural considerations of the snake venom metalloproteinases, key members of the M12 repolysin family of metalloproteinases. *Toxicon* **2005**, *45*, 969–985.
41. Udi, Y.; Fragai, M.; Grossman, M.; Mitternacht, S.; Arad-Yellin, R.; Calderone, V.; Melikian, M.; Toccafondi, M.; Berezovsky, I.N.; Luchinat, C.; et al. Unraveling hidden regulatory sites in structurally homologous metalloproteases. *J. Mol. Biol.* **2013**, *425*, 2330–2346.
42. Takeda, S. Structure-function relationship of modular domains of P-III class snake venom metalloproteinases. In *Venom Genomics and Proteomics*; Gopalakrishnakone, P., Calvete, J.J., Eds.; Springer International Publishing AG: Cham, Switzerland, 2016; pp. 185–209.
43. Takeda, S. ADAM and ADAMTS family proteins and snake venom metalloproteinases: A structural overview. *Toxins* **2016**, *8*, 155.
44. Ito, A.; Mukaiyama, A.; Itoh, Y.; Nagase, H.; Thogersen, I.B.; Enghild, J.J.; Sasaguri, Y.; Mori, Y. Degradation of Interleukin 1-beta by matrix metalloproteinases. *J. Biol. Chem.* **1996**, *271*, 14657–14660.
45. Sisto, M.; Lisi, S.; Lofrument, D.D.; Frassanito, M.A.; Cucci, L.; D'Amore, S.; Mitolo, V.; D'Amore, M. Induction of TNF-alpha-converting enzyme-ectodomain shedding by pathogenic autoantibodies. *Int. Immunol.* **2009**, *12*, 1341–1349.
46. Mohammed, F.F.; Smookler, D.S.; Khokh, A.R. Metalloproteinases, inflammation, and rheumatoid arthritis. *Ann. Rheum. Dis.* **2003**, *62*, 43–47.

47. Bradford, M.M. A rapid and sensitive method for the quantitation of microgram quantities of protein utilizing the principle of protein dye binding. *Anal. Biochem.* **1976**, *72*, 248–254.
48. Marim, F.M.; Silveira, T.N.; Lima, D.S., Jr.; Zamboni, D.S. A method for generation of bone marrow-derived macrophages from cryopreserved mouse bone marrow cells. *PLoS ONE* **2010**, *5*, e15263.
49. Mosmann T. Rapid colorimetric assay for cellular growth and survival: Application to proliferation and cytotoxicity assays. *J. Immunol. Methods.* **1983**, *65*, 55–63.
50. Laemmli, U.K. Cleavage of structural proteins during the assembly of the head of bacteriophage T4. *Nature* **1970**, *227*, 680–689.
51. Towbin, H.; Staehelin, T.; Gordon, J. Electrophoretic transfer of proteins from polyacrylamide gels to nitrocellulose sheets: Procedure and some applications. *Proc. Natl. Acad. Sci. USA* **1979**, *76*, 4350–4354.
52. RCSB Protein Data Bank. Available online: www.pdb.org (accessed on 10 June 2016).
53. ModRefiner. Available online: <http://zhanglab.ccmb.med.umich.edu/ModRefiner> (accessed on 12 June 2016).
54. Cluspro program. Available online: <http://cluspro.bu.edu/login.php> (accessed on 11 June 2016).
55. MetaPocket 2.0. Available online: <http://projects.biotec.tu-dresden.de/metapocket/index.php> (accessed on 10 June 2016).
56. The PDB sum platform. Available online: <http://www.ebi.ac.uk/pdbsum> (accessed on 9 June 2016).
57. Drugscore PPI 2.2. Available online: <http://cpclab.uni-duesseldorf.de/dsppi/main.php> (accessed on 12 June 2016).
58. Platform Prosper. Available online: <https://prosper.erc.monash.edu.au/home.html> (accessed on 10 June 2016).



© 2016 by the authors. Submitted for possible open access publication under the terms and conditions of the Creative Commons Attribution (CC-BY) license (<http://creativecommons.org/licenses/by/4.0/>).

Supplementary Materials: Interaction between TNF and BmooMP-Alpha-I, a Zinc Metalloprotease Derived from *Bothrops moojeni* Snake Venom, Promotes Direct Proteolysis of This Cytokine: Molecular Modeling and Docking at a Glance

Maraisa Cristina Silva, Tamires Lopes Silva, Murilo Vieira Silva, Caroline Martins Mota, Fernanda Maria Santiago, Kelly Cortes Fonseca, Fábio Oliveira, Tiago Wilson Patriarca Mineo and José Roberto Mineo

1. Primary Bone-Marrow-Derived Macrophage (BMDM) Cultures

Macrophages were obtained by differentiation of bone marrow from C57BL/6 mice, by using L929-cell conditioned medium (LCCM), as a source of granulocyte/macrophage colony stimulating factor, as previously described [1]. Cells were resuspended in 10 mL bone marrow differentiation media (R20/30), which is RPMI 1640 supplemented with 20% fetal bovine serum (Gibco, cat. 12657-029, Waltham, MA, USA), 30% LCCM, 100 U/mL penicillin, 100 µg/mL streptomycin, and 2 mM of L-glutamine. Cells were seeded in non-tissue culture treated Optilux Petri dishes (BD Biosciences, San Jose, CA, USA) and incubated at 37 °C in a 5% CO₂ atmosphere. Four days after seeding the cells, an extra 10 mL of fresh R20/30 were added per plate and incubated for an additional 3 days. To obtain the BMDM, the supernatants were removed and the attached cells were washed with 10 mL of sterile PBS. Then, 10 mL of ice-cold PBS were added to each plate and incubated at 4 °C for 10 min. The macrophages were detached by gently pipetting the PBS across the dish. Cells were centrifuged at 200× *g* for 5 min and resuspended in 10 mL of BMDM cultivation media (R10/5), which is composed of RPMI 1640, 10% fetal bovine serum, 5% LCCM and 2 mM of L-glutamine. Cells were counted, seeded and cultivated in tissue culture plates for the experimental procedures.

2. Cellular Viability Assay

Murine macrophages treated with BmooMP-alpha-I or PRR agonist were assessed to determine cellular viability, which was evaluated by MTT assay, as previously described [2]. In the first step, 10 µL of thiazolyl

blue (MTT) was added at a concentration of 5 mg/mL in medium RPMI supplemented with 10% fetal calf serum (SFB), 4 h before the end of culture of BMDM. After the supernatants were removed, the insoluble purple coloured particles produced by viable cells metabolized MTT were solubilized with 100 μ L/well of 10% SDS and 50% *N,N*-dimethyl formamide (DMF). After 30 min incubation, the optical densities were determined in plate reader at 570 nm. The results were expressed as the percentage of viable cells compared to controls.

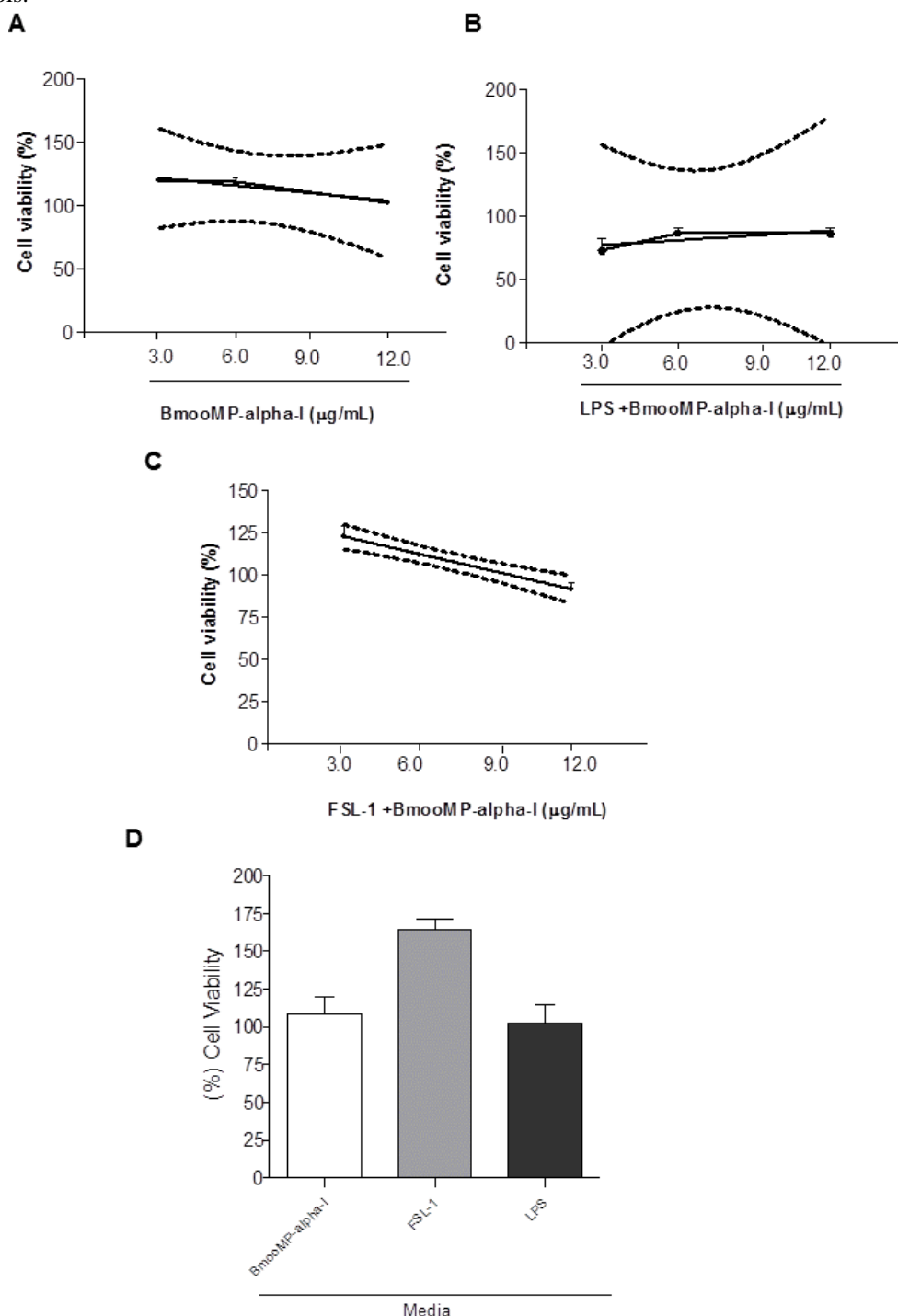


Figure S1. Cell viability determined by MTT assay of macrophages treated with PRR agonists and/or BmoMP- α -I. (A) Cells were cultured in 96-well plates for 24 h and treated with BmoMP- α -I (12 to 1.5 μ g/mL) for additional incubation of 24 h; (B) Cells were cultured in 96-well plates for 24 h, activated for 3 h with agonist of Toll-like receptor (TLR): LPS (1 μ g/mL); (C) Cells were cultured in 96-well plates for 24 h, activated for 3 h with agonist of TLR: FSL-1 (1 μ g/mL). Cells were washed with RPMI, and treated with

BmooMP-alpha-I (12 to 1.5 $\mu\text{g/mL}$) for additional incubation of 24 h; **D**) Cells were cultured in 96-well plates for 24 h and incubated with RPMI medium only (absence of BmooMP-alpha-I) or activated for 3 h with TLR agonists: LPS and FSL-1 for additional incubation with medium of 24 h. The negative control cells were incubated with RPMI medium only. The negative control cells were incubated with RPMI medium only. The results are expressed as mean \pm SD of the percentage of viable cells compared to control and in (A–C) the results are plotted in a non-linear regression represented by a dose response curve with 95% confidence interval.

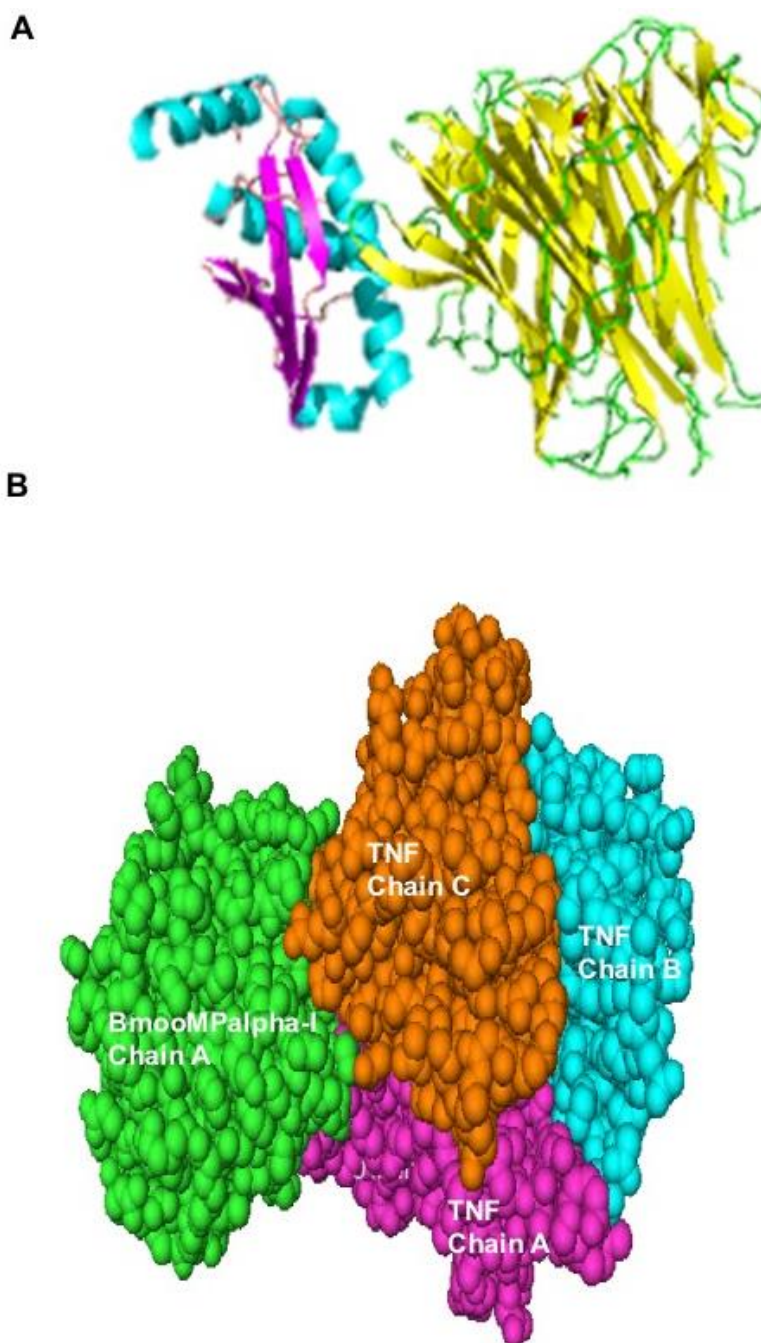


Figure S2. The docking analysis and interacting residues. (A) Structure interaction resulted from CLUSPRO analysis in which BmooMP-alpha-I is represented in blue and magenta, and murine TNF in green and yellow; (B) BmooMP-alpha-I and murine TNF complex in 3D vision determined by PYMOL.

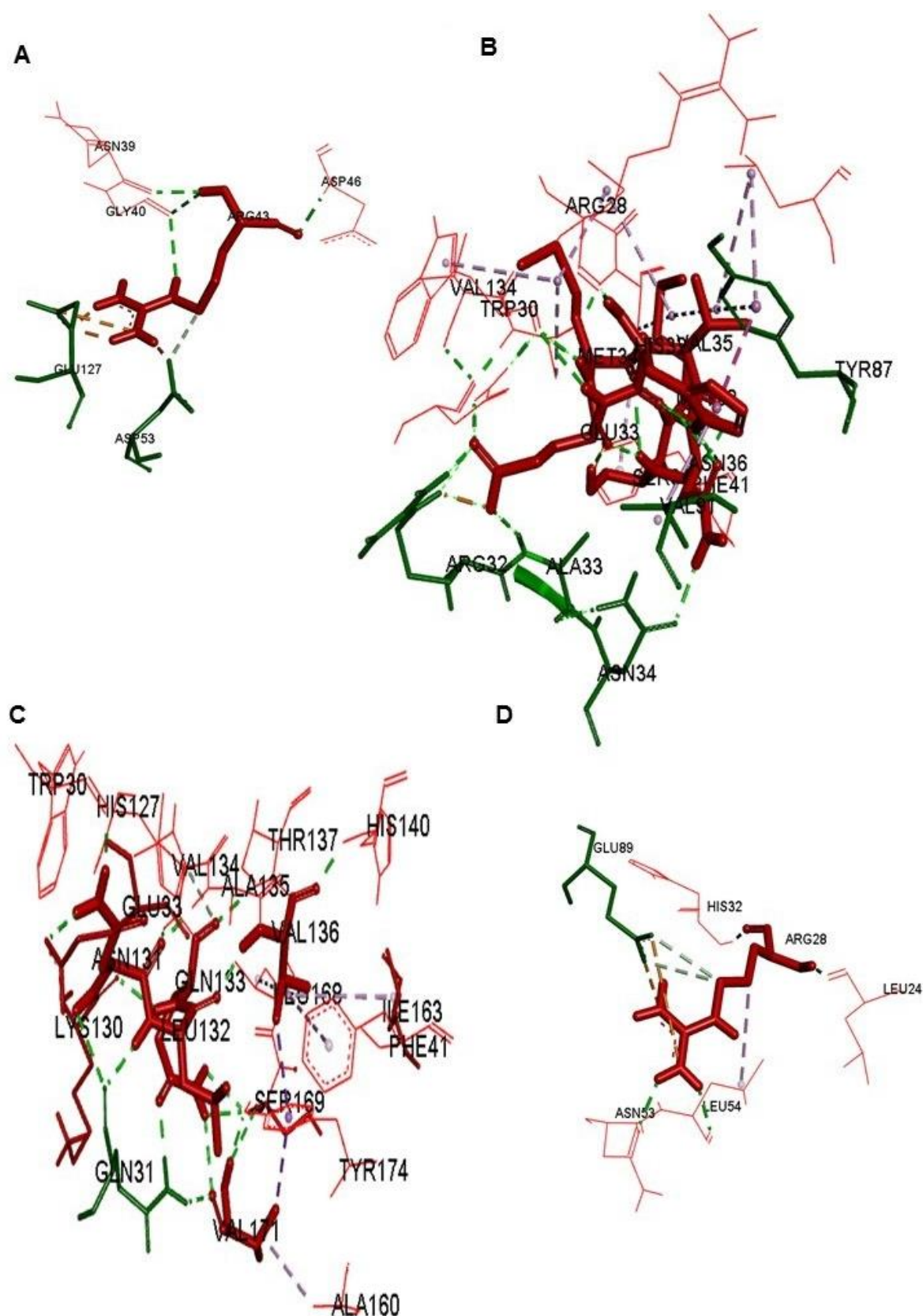


Figure S3. Analysis of the BmooMP-alpha-I and TNF interaction by Discovery Studio 3.5.0. (A–D) Demonstration of interacting residues in zoom out view. BmooMP-alpha-I is represented in red, and murine TNF in green.

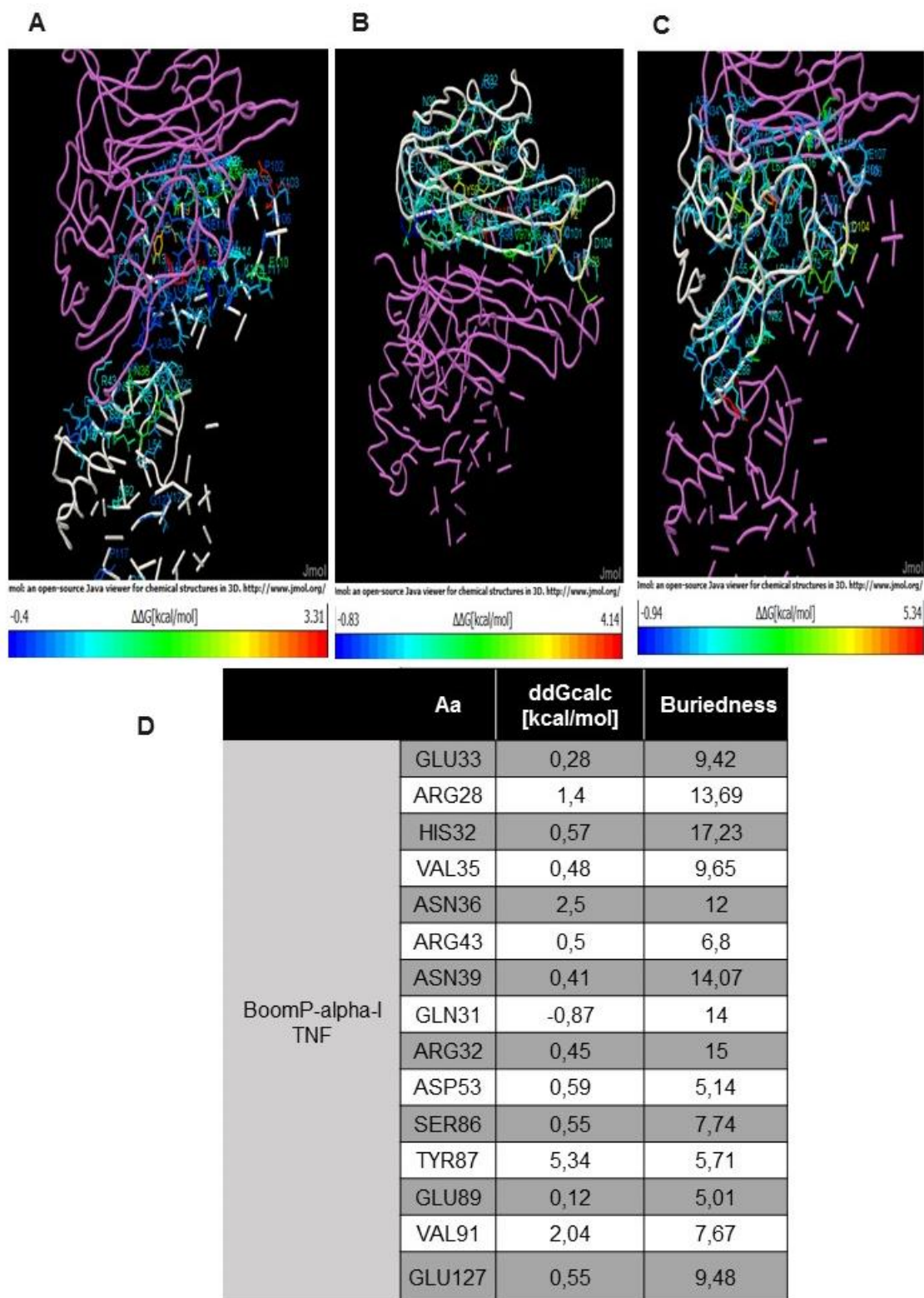


Figure S4. Alanine scanning analysis. Representation of the amino acid residues according to their sidechain's contribution to the binding free energy, as given in the color scale. The chain representations of the TNF for each residue contributions are shown in white, whereas the correspondent chains of the BmooMP-alpha-I are shown in magenta. (A) BmooMP-alpha-I and TNF chain A; (B) BmooMP-alpha-I and TNF chain B; (C) BmooMP-alpha-I and TNF chain C; (D) The relevant residues for interaction between TNF and BmooMP-alpha-I in terms of ddGcalc (kcal/mol).

	INTERACTION	DISTANCE	CATEGORY	TYPE	FROM	FROM CHEMISTRY	TO	TO CHEMISTRY
BmooMP- α -I TNF	A:ALA49:HN - A:ASN39:OD1	1,9549	Hydrogen Bond	Conventional Hydrogen Bond	A:ALA49:HN	H-Donor	A:ASN39:OD1	H-Acceptor
	A:ARG28:CD - C:GLU89:OE1	3,69941	Hydrogen Bond	Carbon Hydrogen Bond	A:ARG28:CD	H-Donor	C:GLU89:OE1	H-Acceptor
	A:ARG43:CD - C:ASP53:OD2	3,48028	Hydrogen Bond	Carbon Hydrogen Bond	A:ARG43:CD	H-Donor	C:ASP53:OD2	H-Acceptor
	A:ARG43:HE - A:GLY40:O	2,8904	Hydrogen Bond	Conventional Hydrogen Bond	A:ARG43:HE	H-Donor	A:GLY40:O	H-Acceptor
	A:ARG43:HH11 - C:GLU127:OE2	1,89545	Hydrogen Bond/Electrostatic	Salt Bridge/Attractive Charge	A:ARG43:HH11	H-Donor;Positive	C:GLU127:OE2	H-Acceptor;Negative
	A:ARG43:HH12 - C:ASP53:OD2	1,85704	Hydrogen Bond/Electrostatic	Salt Bridge/Attractive Charge	A:ARG43:HH12	H-Donor;Positive	C:ASP53:OD2	H-Acceptor;Negative
	A:ARG43:HH21 - C:GLU127:OE2	1,81394	Hydrogen Bond/Electrostatic	Salt Bridge/Attractive Charge	A:ARG43:HH21	H-Donor;Positive	C:GLU127:OE2	H-Acceptor;Negative
	A:ASN39:HD21 - A:VAL35:O	1,96198	Hydrogen Bond	Conventional hydrogen bond	A:ASN39:HD21	H-Donor	A:VAL35:O	H-Acceptor
	A:ASN39:HD22 - A:ALA49:O	2,09801	Hydrogen Bond	Conventional hydrogen bond	A:ASN39:HD22	H-Donor	A:ALA49:O	H-Acceptor
	A:GLN31:HE21 - A:VAL171:O	2,25929	Hydrogen Bond	Conventional hydrogen bond	A:GLN31:HE21	H-Donor	A:GLN133:O	H-Acceptor
	A:GLN31:HE21 - A:GLN133:OE1	1,90048	Hydrogen Bond	Conventional hydrogen bond	A:GLN31:HE21	H-Donor	A:GLN133:OE1	H-Acceptor
	A:GLY40:O - A:ASP42:N	3,24861	Hydrogen Bond	Conventional hydrogen bond	A:GLY40:O	H-Donor	A:ASP42:N	H-Acceptor
	A:HIS32 - C:TYR87	3,56997	Hydrophobic	PI-PI stacked	A:HIS32	PI-Orbitals	C:TYR87	PI-Orbitals
	A:HIS32 - C:VAL91	3,90316	Hydrophobic	PI-Alkyl	A:HIS32	PI-Orbitals	C:VAL91	Alkyl
	A:TYR42:HN1 - A:ASN39:O	2,31259	Hydrogen Bond	Conventional Hydrogen Bond	A:TYR42:HN1	H-Donor	A:ASN39:O	H-Acceptor
	A:VAL136:HN1 - A:LEU132:O	2,34701	Hydrogen Bond	Conventional Hydrogen Bond	A:VAL136:HN1	H-Donor	A:LEU132:O	H-Acceptor
	C:SER86:CB - A:ALA49:O	2,9638	Hydrogen Bond	Carbon Hydrogen Bond	C:SER86:CB	H-Donor	A:ALA49:O	H-Acceptor
	C:SER86:HG - A:ASN39:OD1	4,40404	Hydrogen Bond	PI-Alkyl	C:TYR87	PI-Orbitals	A:LEU51	Alkyl
	A:ASN36:HD21 - A:ASN34:OD1	2,02225	Hydrogen Bond	Conventional Hydrogen Bond	A:ASN36:HD21	H-Donor	A:ASN34:OD1	H-Acceptor
	A:ARG32:HE - A:GLU33:OE2	2,00538	Hydrogen Bond	Conventional Hydrogen Bond	A:ARG32:HE	H-Donor	A:GLU33:OE2	H-Acceptor
	A:ALA33:HN - A:GLU33:OE2	2,09645	Hydrogen Bond	Conventional Hydrogen Bond	A:ALA33:HN	H-Donor	A:GLU33:OE2	H-Acceptor
	C:TYR87 - A:VAL35	4,73482	Hydrogen Bond	PI-Alkyl	B:TYR87	PI-Orbitals	A:VAL35	Alkyl

Figure S5. Interaction between the residues of BmooMP- α -I and TNF. Interaction specifications between BmooMP- α -I and TNF were obtained by Discovery Studio 3.5.0. The letter in front of the residue indicates the chain of the molecules.

References

1. Marim, F.M.; Silveira, T.N.; Lima, D.S., Jr.; Zamboni, D.S. A method for generation of bone marrow-derived macrophages from cryopreserved mouse bone marrow cells. *PLoS ONE* **2010**, *5*, e15263.
2. Mosmann, T. Rapid colorimetric assay for cellular growth and survival: Application to proliferation and cytotoxicity assay. *J. Immunol. Methods* **1983**, *65*, 55

Capítulo II: SILVA, M.C *et al.* 2019

**Treatment with a zinc metalloprotease purified from *Bothrops moojeni* snake venom
(BmooMP-alpha-I reduces the inflammation in an experimental model of dextran sulfate
sodium-induced colitis**

Maraisa Cristina Silva¹, Helioswilton Sales-Campos^{2,3}, Carlo José Freire de Oliveira², Tamires
Lopes Silva¹, Flávia Batista Ferreira França¹, Fábio Oliveira⁴, Tiago Wilson Patriarca Mineo¹,
José Roberto Mineo^{1,*}

¹ Laboratório de Imunoparasitologia Dr. Mário Endsfieldz Camargo, Instituto de Ciências
Biomédicas, Universidade Federal de Uberlândia, 38400-902 Uberlândia, MG, Brazil

² Laboratório de Imunologia, Instituto de Ciências Biológicas e Naturais, Universidade Federal
do Triângulo Mineiro, 38025-180, Uberaba, MG, Brazil

³ Departamento de Biociências e Tecnologia, Instituto de Patologia Tropical e Saúde Pública,
Universidade Federal de Goiás, 74605-050, Goiânia, GO, Brazil

⁴ Laboratório de Biofísica, Instituto de Ciências Biomédicas, Universidade Federal de
Uberlândia, 38400-902 Uberlândia, MG, Brazil and Instituto Nacional de Ciência e Tecnologia
em Nano-Biofarmacêutica (N-Biofar), 31270-901 Belo Horizonte, MG, Brazil

* Corresponding author

Email: jrmineo@ufu.br - Phone: 55-34-99815-3133

Abstract

It has been described that the metalloprotease BmooMP-alpha-I purified from *Bothrops moojeni* snake venom is able to hydrolyze the TNF molecule. However, this observation has been based mainly on *in vitro* investigation, in addition to molecular modeling and docking approaches. Considering that there is no *in vivo* study to demonstrate the biological effects of this enzyme, the major aim to the present work was to investigate whether the BmooMP-alpha-I has any the anti-inflammatory efficacy by setting up a murine experimental design of colitis induced by dextran sulfate sodium (DSS). For this purpose, C57BL/6 mice were divided into six groups, as follows: i.) animals without intestinal inflammation; ii.) animals without intestinal inflammation treated with BmooMP-alpha-I (50 µg/animal/day); iii.) animals with intestinal inflammation induced by 3% of DSS; iv.) mice with intestinal inflammation induced by DSS and treated with BmooMP-alpha-I enzyme at the 50, 25 or 12.5 µg/animal/day dosages by intraperitoneal route. Clinical signs of colitis were daily observed for calculating the morbidity scores, cytokine measurements and histological features. We observed that the animals treated with different doses of the enzyme presented a remarkable improvement of colitis signs, as confirmed by a significant increase of the intestine length in comparison to DSS group. Also, no difference was observed between the groups treated with the enzyme or vehicle, as the colon length of these animals was slightly lower than the group of healthy animals, without induction of intestinal inflammation. The cytokine quantification in supernatants of intestinal tissue homogenates showed a significant reduction of 38% in IFN-gamma levels, when the animals was treated with 50 µg of the BmooMP-alpha-I compared to the animals receiving DSS only. A significant reduction of 39% in TNF levels was also observed in all doses of treatment with BmooMP-alpha-I, in addition to a significant reduction of 35% in the amount of IL-12p40. Histological examinations revealed that the BmooMP-alpha-I 50 µg treated group preserved colon architecture and goblet cells and reduced the ulcer area, when compared with DSS mice, which showed typical inflammatory changes in tissue architecture, such as ulceration, crypt dilation, loss of tissue architecture, and goblet cell depletion, accompanied by a significant cell infiltration. In conclusion, our results suggest that the improvement of clinical scores and histological findings related to BmooMP-alpha-I treatment in this experimental model could be attributed to the metalloprotease ability to modulate cytokine production locally at the inflamed intestine. These findings highlight the potential anti-inflammatory role and effectiveness of this enzyme as therapeutic alternative in this type of immunopathological

condition.

1. Introduction

Inflammatory bowel diseases (IBD), as ulcerative colitis (UC) and Crohn's disease (CD), are chronic inflammatory disorders identified by an imbalance between inflammatory and regulatory immune responses at the gut mucosa [1]. The incidence of inflammatory bowel diseases has increased worldwide and it is now estimated that between 1 and 1.3 million of Americans are currently diagnosed with IBD [2-4]. This increased incidence is possibly due to currently unidentified environmental factors, which interact with an inherent genetic predisposition and immune dysregulation [4-6]. Ulcerative colitis (UC) is an intestinal inflammation that presents an extensive damage of colon mucosa. The various clinical manifestations with attacks of abdominal cramps, pain, bloody diarrhea, bleed per rectum, weight loss, fever, and easy fatigability, may begin gradually or start totally all at once [5-7]. These clinical manifestations interfere notably in the quality of life of affected patients [8].

Cytokines have a crucial role in the pathogenesis of IBD, because these immunological markers are able to guide multiple aspects of the inflammatory response and they are associated with the clinical symptoms. The combination of genetic and environmental characteristics is necessary to initiate alterations in epithelial barrier function, thereby leading to the translocation of luminal pathogens or even components from commensal microbiota into the bowel wall. Subsequently, unbalanced cytokine responses in such microenvironmental niche trigger subclinical or acute mucosal inflammation mostly in genetically susceptible hosts. In patients that fail to control the acute intestinal inflammation, chronic intestinal inflammation develops, which is result of an uncontrolled activation of the mucosal immune system. Furthermore, cytokines seem to have a crucial role in the pathogenesis of progressive and destructive forms of IBD, being associated with complications such as intestinal stenosis, rectal bleeding, abscess and fistula formation, and the development of colitis-associated neoplasia [9].

Pharmacological and/or biological treatment strategies for IBD are used in the clinical management of the patients, which include aminosalicylates, corticosteroids, apremilast, cytokine inhibitors (as IL-6–IL-6R or IL-12–IL-23), modulators of cytokine signaling events (as JAK inhibitors or SMAD7 blocker), inhibitors of transcription factors (as GATA3 or ROR γ t), anti-T-cell-activation and anti-migration factors (as β 7 integrin), or TNF blockers (anti-TNF antibodies) [10,11]. However, all these strategies are not totally effective and a significant number of patients requires repeated intestinal surgeries to control the disease complications. Moreover, some of them are refractory to the pharmacological interventions,

which may also induce severe side effects [12-13]. In view of this, the investigations of new therapies that combine efficacy, effective dosing, and fewer adverse effects are important goal for human IBD therapy. In this regard, the use of alternative therapies has emerged as a helpful approach to treat this type of gastrointestinal diseases, because it has been described that almost half of the IBD patients have attempted or presently use alternative therapies [13-14]. In fact, there are different complementary therapies, such as the use of bioactive factors, particularly those derived from plants and animals, that can modulate the microenvironment of intestinal inflammation [15-17] and the experimental colitis models have been used to identify this type of therapeutic agents and elucidate the underlying physiologic mechanisms of IBD. In this context, the major aim of the present study was to examine the effect of a zinc metalloprotease derived from *Bothrops moojeni* snake venom (BmooMP-alpha-I) as a potential therapeutic agent to treat intestinal inflammation in a murine model of colitis induced by dextran sulfate sodium, considering that this enzyme can interfere in the TNF biological function by directly promoting its hydrolysis.

2. Materials and Methods

2.1 Animals

C57BL/6 male mice (18-22 g/6–8 weeks old) were housed at the Center of Bioterism and Animal Experimentation from Universidade Federal de Uberlândia (CBEA-UFU) in temperature-controlled rooms, receiving water and food *ad libitum* throughout the experimental conditions. This study was approved by the Ethical Committee for Animal Experimentation from Universidade Federal do Triângulo Mineiro (CEUA-UFTM) (Protocol # 372/16, from April 29, 2016), in accordance with the procedures established by the Universities Federation for Animal Welfare (UFAW).

2.2 Purification and biochemical characterization of BmooMP-alpha-I

The metalloprotease BmooMP-alpha-I was isolated and purified and its biological activity was assessed, as previously described [18]. The purified enzyme was diluted, dialyzed against 50 mM ammonium bicarbonate (pH 7.8), lyophilized, and stored at -20 °C until used. Protein concentration was determined by the Bradford method [19].

2.3 Experimental and control groups in DSS-induced colitis

Experimental design for DCC-induced colitis was carried out according with our previous work [20]. Mice were allocated into six groups with six animals each, as follows: animals without intestinal inflammation (negative control group); animals without intestinal inflammation treated with BmooMP-alpha-I (50 µg/animal/day) (treatment control group); animals with intestinal inflammation induced by 3% DSS (M.W. 36,000-50,000, MP Biomedicals, Illkirch, France), treated with the diluent only (PBS) (vehicle group); and mice with intestinal inflammation induced by DSS and treated with BmooMP-alpha-I enzyme at the doses of 50, 25 or 12.5 µg/animal/day (treatment groups). Each mouse from all groups was identified on its tails by nontoxic pen. Mice from model control group were exposed to 3% (w/v) DSS in drinking water during 6 consecutive days. After being exposed to DSS for 6 days, mice from treatment groups were treated intraperitoneally (i.p.) with BmooMP-alpha-I and euthanized at day 6 after the beginning of DSS exposure. Animals from control groups were treated with vehicle only during 6 days (Figure 1A).

2.4 Clinical signs and score determinations

Clinical signs of colitis were determined, as previously described by our group [20]. Briefly, the following parameters were evaluated: weight loss; wet anus; diarrhea; bleeding stools; hypoactivity and piloerection. The disease scores were evaluated according with the same criteria defined in our previous work [20]. Mice were euthanized at day 6 after colitis induction and the intestines were collected for further analysis. Intestinal tissues were immediately frozen in liquid nitrogen in the presence of a protease inhibitor cocktail (Complete®, Roche, Pharmaceuticals, Mannheim, Germany) for myeloperoxidase (MPO) activity.

2.5 Cytokine measurements

After euthanasia, colon was portioned in 4 pieces weighting 60 mg/each in average. To facilitate comparison of data between mice and groups, the same portions were used for each determination. TNF was quantified using a commercial ELISA kit (R&D Systems, Minneapolis, MN, USA). Also, the levels of IL-12p40 and IFN-gamma production were determined in these samples, using appropriate kits (BD, Franklin Lakes, NJ, USA). The cytokine concentrations in the intestinal samples were determined in accordance with the manufacturer's instructions.

2.6 MPO Assay

Fragments from colon were cut into small pieces, weighed and processed for MPO quantification, as previously described [21], with modifications. Briefly, for MPO assay, fragments were homogenized and erythrocytes were lysed. The pellets obtained after centrifugation were resuspended, followed by three freezing and thawing rounds. After centrifugation, the supernatants were transferred to 96-well plates and the MPO measurements were carried out by addition of TMB Substrate Reagent Set (Tetramethylbenzidine – BD OptEIA™, San Diego, CA) at 37°C. The reaction was stopped and readings were performed in a spectrophotometer at 450 nm. The results were expressed as optical density per gram of tissue.

2.7 Histology and histopathological analysis

To observe the effect of the metalloprotease treatment in the DSS-induced colitis, the intestinal tissues from all groups of animals were obtained and analyzed, as previously described [20]. Briefly, the final portions of colon were opened longitudinally for assessment of macroscopic damage. These tissues were rinsed in PBS, placed in 10% buffered formalin for 24 h and processed to be embedded in paraffin. Tissue sections of 5 µm were acquired and processed for hematoxylin and eosin stained. Images were obtained at 20 x magnification in FSX100 Olympus Microscopy.

2.8 Statistical analysis

Data were analyzed by using GraphPad Prism software (La Jolla, CA, USA). As the results showed normal distribution, it was performed the one-way Anova test followed Bonferroni post-hoc test. The results are representative from at least three independent experiments, and the statistical analysis was based on 6 animals per group. Values of $p < 0.05$ were considered significant.

3. Results

To evaluate whether the BmooMP-alpha-I enzyme would be able to interfere in the colitis inflammatory signs, C57BL/6 mice were treated with 50, 25 or 12.5 µg/animal/day by intraperitoneal route by intraperitoneal route of the enzyme and the disease clinical outcome was evaluated as described in the design experimental (Figure 1A). Even though significant difference was not observed under macroscopic evaluation of the intestine at the time of

1 euthanasia (Figure 1B), the clinical signs showed marked improvements, as the animals treated
2 with the highest enzyme dose increased the colon length, which was similar to that observed in
3 the vehicle treated group, or in the other doses tested. Also, no difference was observed
4 between the groups treated with the enzyme or vehicle, as the colon length of these animals was
5 slightly lower than the group of healthy animals, without induction of intestinal inflammation
6 (Figure 1C). Additionally, we showed that mice treated the highest dose of BmooMP-alpha-I
7 showed a tendency to reduce the clinical score, post-mortem score and accumulated score when
8 compared to the other groups (Figure 2A-C). The beneficial effect the highest dosage of
9 BmooMP-alpha-I was confirmed by the overall score, which represents clinical condition of the
10 mice during all period of the experimental observation, considering that significant differences
11 were observed among the treated groups and colitis group (Figure 2D).

12 To assess the effect of BmooMP-alpha-I in the production of pro-inflammatory cytokines and
13 myeloperoxidase (MPO) activity, additional experiments were performed. The cytokine
14 measurements in the supernatants of intestinal tissue homogenates showed a significant
15 reduction of 38.0% in IFN- gamma levels, when the animals were treated with 50
16 µg/animal/day of the BmooMP-alpha-I compared to the animals receiving DSS only (Figure
17 3A). Also, it was observed significant reductions of the TNF levels in the animals treated with
18 BmooMP-alpha-I in all doses tested, with a reduction average 38.9% compared to the DSS-
19 induced colitis group (Figure 3B). Furthermore, the highest dose of BmooMP- alpha-I was also
20 able to significantly reduce in 35.0% the amount of IL-12p40 (Figure 3C).

21 On the other hand, the measurements of MPO levels demonstrated that the animals with colitis
22 and treated BmooMP-alpha-I were not statistically significant compared to the untreated DSS-
23 induced colitis group. Overall, these results suggested that the improvement of clinical scores
24 related to the BmooMP-alpha-I therapy could be attributed to its ability to modulate cytokine
25 production locally at the inflamed intestine.

26 Histological analyses of the colon revealed that DSS mice showed typical inflammatory
27 changes in colon morphology, characterized by crypt dilation, goblet cell depletion and
28 inflammatory cell infiltration, resulting in a significant loss of tissue architecture. Compared to
29 the DSS group, mice treated with the BmooMP-alpha-I highest dose presented ameliorated
30 histological aspect of the tissue and reduced inflammatory signs. The enzyme did not cause
31 tissue damage, presenting the same aspect of the negative control group (Figure 4A-D).

4. Discussion and conclusions

The inflammatory disorders affecting the intestinal tissues, as ulcerative colitis and Crohn's disease, remain as severe gastrointestinal diseases to be solved [22, 23]. Currently, therapeutic advances have led to a paradigm shift in the clinical management of patients with IBD. The introduction of immunosuppressive or biologic agents, such as azathioprine or TNF blockers, has markedly reduced the need to use corticosteroids for therapy [24–26]. However, one of the most investigated approaches that has been described is based on the treatment with antibodies directed to TNF. Currently, monoclonal antibodies against TNF are commercially available to treat TNF-mediated pathologies. In fact, these antibodies are also frequently applied for treatment of rheumatoid arthritis, in addition to promising results that have been obtained for treatment of other inflammatory disorders [22, 23]. Concerning the inflammatory diseases affecting the intestinal tissues, however, the anti-TNF antibody therapy has been described to be moderately effective during clinical management of the patients. Indeed, there are several observations pointing out that not all patients respond to the anti-TNF therapy, besides the fact that this therapeutic option has been associated with serious side-effects [27]. TNF is a classical pro-inflammatory cytokine involved in the modulation of acute inflammatory responses and host defense mechanisms [27]. It is mainly produced by monocytes and secreted as a transmembrane protein (mTNF-26 kDa) and cleaved by the TNF-converting enzyme (TACE), a zinc metalloprotease, in its soluble form (sTNF-17 kDa). Both fragments are biologically active and bind as trimers to both TNFR1 and TNFR2 receptors [28]. However, it is necessary to pointing out that TNF has pleiotropic effects in the bowel wall: it induces neoangiogenesis; activates macrophages to produce proinflammatory cytokines; favors Paneth cell death via necroptosis; augments apoptosis of intestinal epithelial cells; regulates T-cell apoptosis; and reduces production of tissue inhibitor of matrix metalloproteinases (MMPs) by fibroblasts to mediate tissue injury via activated MMPs. Thus, anti-TNF antibodies can suppress intestinal inflammation in IBD through several mechanisms [9, 29].

In our previous study, we investigated the role of BmooMP-alpha-I as a biological product able to hydrolyze the TNF cytokine, based mainly on in vitro experiments, as well as on modeling and docking approaches [18]. We concluded that this metalloprotease could be used to modulate of the inflammatory response, but this application would require further investigation, particularly when tested to treat inflammatory disorders involving TNF cytokine. Consequently, in the present study we advanced in the process to characterize this metalloprotease as modulator of the inflammatory response, by using an in vivo experimental design already applied in our

group to assess an experimental inflammatory of bowel disease [20]. Therefore, when compared with our previous studies [18, 20], it is necessary to emphasize that the present work investigated for the first time the use of the BmooMP-alpha-I metalloprotease to treat DSS-induced colitis.

The efficacy of the BmooMP-alpha-I was assessed by setting up a murine experimental design of colitis induced by DSS. The clinical signs of colitis were daily observed for calculating the disease scores and it was found that the animals treated with different doses of this enzyme presented a marked improvement of colitis signs, as observed by an increase in the intestine length. Also, no difference was observed between the groups treated with the enzyme or vehicle, as the colon length of these animals was slightly lower than the group of healthy animals, without induction of intestinal inflammation. The association between exposure to DSS and decrease in the bowel length constitutes an important piece of information [30, 31] and this parameter has been recently reinforced in the literature, demonstrating the colon length as a well-established indicator of DSS-induced colitis, particularly when the colon shortening is examined after 7 days of DSS treatment. In the present work, as predictable, DSS treatment resulted in colon shortening, whereas the group of animals treated with BmooMP-alpha-I significantly improved such indicator of inflammatory response.

The cytokine quantification in supernatants of the intestinal tissue homogenates showed a significant reduction of 39% in TNF levels when the treatment with BmooMP-alpha-I was performed. A significant reduction of 38% in IFN-gamma levels was also observed, when the animals was treated with 50 µg of the BmooMP-alpha-I compared to the animals receiving DSS only. In addition, a significant reduction of 35% in the amount of IL-12 was also observed in our DSS induce colitis, even though it has been described that the effect of the BmooMP-alpha-I metalloprotease on TNF is independent of cell cytotoxicity and it does not affect other TLR triggered cytokines, such as IL-12p40 [32].

Histological examinations revealed that in the group treated with 50 µg of BmooMP-alpha-I preserved colon architecture and goblet cells and reduced the ulcer area, when compared with DSS mice, which showed typical inflammatory changes in the tissue morphology, such as crypt dilation, loss of tissue architecture, and goblet cell depletion, accompanied by a significant cell infiltration.

Metalloproteases represent at least 30% of the toxin composition of many viperid snake venoms and they are responsible for hemorrhage through disturbances in the blood coagulation cascade of prey and snakebite victims [33]. However, certain metalloproteases lack hemorrhagic activity, but present other biological effects, such as inhibition of platelet aggregation, induction of

apoptosis, and pro- or anti-inflammatory activities [34-35]. Previous study of the crystal structure of BmooMP-alpha-I showed that the enzyme presents a catalytic zinc ion displaying an unusual octahedral coordination, which includes three canonical histidines [36]. In the present work, we clearly demonstrated that the treatment with BmooMP-alpha-I metalloprotease could impair the inflammatory response in the DSS-induced colitis experimental design. In summary, our results suggest that the improvement of clinical scores and histological findings related to BmooMP-alpha-I treatment in this experimental model could be attributed to the metalloprotease ability to modulate cytokine production locally at the inflammatory intestinal microenvironment. We conclude that these findings could provide a novel perspective to treat intestinal inflammatory diseases, highlighting the potential anti-inflammatory role of this metalloprotease and its effectiveness as therapeutic alternative in this type of immunopathological condition.

Data Availability

The data used to support the findings of this study are available from the corresponding author upon request.

Conflict of Interests

The authors declare that there is no conflict of interests regarding the publication of this paper.

Acknowledgments

This study was financially supported by Brazilian research agencies (Fundação de Amparo à Pesquisa do Estado de Minas Gerais-FAPEMIG, Grant # RED-00013-14 and #APQ-01313-14; Conselho Nacional de Desenvolvimento Científico e Tecnológico (CNPq, Brazil) Grant # 311787/2013-4 and 456650/2013-0; Coordenação de Aperfeiçoamento de Pessoal de Nível Superior-CAPES, Grant #AUXPE-02450/09-7). JR, NS, CO and TW receive research fellowships from Conselho Nacional de Desenvolvimento Científico e Tecnológico (CNPq, Brazil). TL and FF are recipients of PhD scholarships from Coordenação de Aperfeiçoamento de Pessoal de Nível Superior (CAPES, Brazil).

References

1. X. R. Xu, C. Q. Liu, B. S. Feng, and Z. J. Liu, “Dysregulation of mucosal immune response in pathogenesis of inflammatory bowel disease,” *World J Gastroenterol* **20**, 3255–3264, doi: 10.3748/wjg.v20.i12.3255 (2014).
2. M. D. Kappelman, S. L. Rifas-Shiman, K. Kleinman, D. Ollendorf, A. Bousvaros, R. J. Grand, and J. A. Finkelstein, “The prevalence and geographic distribution of Crohn’s disease and ulcerative colitis in the United States,” *Clin Gastroenterol Hepatol* **5**, 1424– 1429, doi: 10.1016/j.cgh.2007.07.012 (2007).
3. E. V. Loftus, “Clinical epidemiology of inflammatory bowel disease: Incidence, prevalence, and environmental influences,” *Gastroenterology* **126**, 1504–1517, doi: 10.1053/j.gastro.2004.01.063 (2004).
4. S. B. Hanauer, “Inflammatory bowel disease: epidemiology, pathogenesis, and therapeutic opportunities,” *Inflamm Bowel Dis* **12** Suppl 1, S3–S9 doi: 10.1097/01.MIB.0000195385.19268.68 (2006).
5. B. W. Megna, P. R. Carney, and G. D. Kennedy, “Intestinal inflammation and the diet: Is food friend or foe?,” *World J Gastrointest Surg* **8**, 115–123, doi: 10.4240/wjgs.v8.i2.115 (2016).
6. P. J. Basso, M. T. C. Fonseca, G. Bonfá, V. B. F. Alves, H. Sales-Campos, V. Nardini, and C. R. B. Cardoso, “Association among genetic predisposition, gut microbiota, and host immune response in the etiopathogenesis of inflammatory bowel disease,” *Braz J Med Biol Res* **47**, 727–737, doi: 10.1590/1414-431X20143932 (2014).
7. M. Balaha, S. Kandeel, and W. Elwan, “Garlic oil inhibits dextran sodium sulfate- induced ulcerative colitis in rats,” *Life Sci* **146**, 40–51, doi: 10.1016/j.lfs.2016.01.012 (2016).
8. X. Li, Y. Xu, C. Zhang, L. Deng, M. Chang, Z. Yu, and D. Liu, “Protective effect of calculus bovis sativus on dextran sulphate sodium-induced ulcerative colitis in mice,” *Evid Based Complement Alternat Med* **2015**, 469506, doi: 10.1155/2015/469506 (2015).
9. M. F. Neurath. “Cytokines in inflammatory bowel disease” *Nat Rev Immunol* **14**, 329–342, doi:10.1038/nri3661 (2014).

10. M. F. Neurath. “Current and emerging therapeutic targets for IBD” *Nat. Rev. Gastroenterol. Hepatol* **14**, 269–278, doi:10.1038/nrgastro.2016.208 (2017).
11. M. Rodriguez-Canales, R. Jimenez-Rivas, R. M. M. Canales-Martinez, A. J. Garcia- Lopez, N. Rivera-Yañez, O. Nieto-Yañez, Y. Ledesma-Soto, L. E. Sanchez-Torres, M. Rodriguez-Sosa, L. I. IgnacioTerrazas, and M. A. Rodriguez-Monroy, “Protective effect of *Amphipterygium adstringens* extract on dextran sulphate sodium-induced ulcerative colitis in mice,” *Mediators Inflamm* **2016**, 8543561, doi: 10.1155/2016/8543561 (2016).
12. H. Sales-Campos, P. J. Basso, V. B. F. Alves, M. T. C. Fonseca, G. Bonfá, V. Nardini, and C. R. Cardoso, “Classical and recent advances in the treatment of inflammatory bowel diseases,” *Braz J Med Biol Res* **48**, 96–107, doi: 10.1590/1414-431X20143774 (2015).
13. F. Algieri, A. Rodriguez-Nogales, N. Garrido-Mesa, P. Zorrilla, N. Burkard, I. Pischel, H. Sievers, B. Benedek, B. Feistel, B. Walbroel, M. E. Rodriguez-Cabezas, and J. Galvez, “Intestinal anti-inflammatory activity of the *Serpylli herba* extract in experimental models of rodent colitis,” *J Crohn’s Colitis* **8**, 775–788, doi: 10.1016/j.crohns.2013.12.012 (2014).
14. C. A. Siegel, “Review article: explaining risks of inflammatory bowel disease therapy to patients,” *Aliment Pharmacol Ther* **33**, 23–32. doi: 10.1111/j.1365-2036.2010.04489.x (2011).
15. R. J. Hilsden, M. J. Verhoef, H. Rasmussen, A. Porcino, and J. C. Debruyn, “Use of complementary and alternative medicine by patients with inflammatory bowel disease,” *Inflamm Bowel Dis* **17**, 655–662, doi: 10.1002/ibd.21360 (2011).
16. A. V. Weizman, E. Ahn, R. Thanabalan, W. Leung, K. Croitoru, M. S. Silverberg, A. H. Steinhart, and G. C. Nguyen, “Characterization of complementary and alternative medicine use and its impact on medication adherence in inflammatory bowel disease,” *Aliment Pharmacol Ther* **35**, 342–349, doi: 10.1111/j.1365-2036.2011.04956.x (2012).
17. V. Valatas, M. Vakas, and G. Kolios, “The value of experimental models of colitis in predicting efficacy of biological therapies for inflammatory bowel diseases,” *Am J. Physiol Gastrointest Liver Physiol* **305**, G763–G785, doi: 10.1152/ajpgi.00004.2013 (2013).
18. M. C. Silva, T. Lopes-Silva, M. V. Silva, C. M. Mota, F. M. Santiago, K. C. Fonseca, F. Oliveira, T. W. Mineo, and J. R. Mineo, “Interaction between TNF and BmooMP- α -I, a zinc metalloprotease derived from *Bothrops moojeni* snake venom, promotes direct

1 proteolysis of this cytokine: molecular modeling and docking at a glance,” *Toxins* **8**, E223,
2 doi: 10.3390/toxins8070223 (2016).

3 19. M. M. Bradford, “A rapid and sensitive method for the quantitation of microgram quantities
4 of protein utilizing the principle of protein dye binding,” *Anal Biochem* **72**, 248–254 (1976).

5 20. H. Sales-Campos, P. R. de Souza, P. J. Basso, A. D. Ramos, V. Nardini, J. E. Chica, M. L.
6 Capurro, A. Sá-Nunes, and C. R. de Barros Cardoso. “*Aedes aegypti* salivary gland extract
7 ameliorates experimental inflammatory bowel disease,” *Int Immunopharmacol* **26**, 13-22
8 (2015).

9 21. S. Videla, J. Vilaseca, C. Medina, M. Mourelle, F. Guarner, A. Salas, and J. R. Malagelada.
10 “Selective inhibition of phosphodiesterase-4 ameliorates chronic colitis and prevents
11 intestinal fibrosis,” *J Pharmacol Exp Ther* **316**, 940-945 (2006).

12 22. B. Osta, G. Benedetti, and P. Miossec, “Classical and paradoxical effects of TNF-alpha on
13 bone homeostasis,” *Front Immunol* **5**, 1–9, doi: 10.3389/fimmu.2014.00048 (2014).

14 23. D. Wallach, “The cybernetics of TNF: old views and newer ones,” *Semin Cell Dev Biol* **50**,
15 105– 114, doi: 10.1016/j.semcdb.2015.10.014 (2016).

16 24. V. Ramseyer, and J. L. Garvin, “Tumor necrosis factor alpha: regulation of renal function
17 and blood pressure,” *Am J Physiol Renal Physiol* **304**, 1231–1242, doi:
18 10.1152/ajprenal.00557.2012 (2013).

19 25. Z. L. Zhang, H. Y. Fan, M. Y. Yang, Z. K. Zhang, and K. Ke Liu, “Therapeutic effect of a
20 hydroxynaphthoquinone fraction on dextran sulfate sodium-induced ulcerative colitis,”
21 *World J Gastroenterol* **20**, 15310–15318, doi: 10.3748/wjg.v20.i41.15310 (2014).

22 26. Y. Guo, Y. Liu, C. Zhang, Z. Y. Su, W. Li, M. T. Huang, and A. N. Kong, “The epigenetic
23 effects of aspirin: the modification of histone H3 lysine 27 acetylation in the prevention of
24 carcinogenesis process located at the colon in azoxymethane- and dextran sulfate sodium-
25 treated CF-1 mice,” *Carcinogenesis* **37**, 616–624, doi: 10.1093/carcin/bgw042 (2016).

26 27. S. Toden, A. L. Theiss, X. Wang, and A. Goel, “Essential turmeric oils enhance anti-
27 inflammatory efficacy of curcumin in dextran sulfate sodium-induced colitis,” *Sci Rep* **11**,
28 814, doi: 10.1038/s41598-017-00812-6 (2017).

28. J. A. Katz, “Advances in the medical therapy of inflammatory bowel disease,” *Curr Opin Gastroenterol* **18**, 435–440 (2002).
29. K. A. Papadakis, and S. R. Targan, “Role of cytokines in the pathogenesis of inflammatory bowel disease.” *Annu Rev Med* **51**, 289–298, doi:10.1146/annurev.med.51.1.289 (2000).
30. C. Stevens, G. Walz, C. Singaram, M. L. Lipman, B. Zanker, A. Muggia, D. Antonioli, M. A. Peppercorn, and T. B. Strom, “Tumor necrosis factor-alpha, interleukin-1 beta, and interleukin-6 expression in inflammatory bowel disease,” *Dig Dis Sci* **37**, 818–826 (1992).
31. Y. Guo, Y. Liu, C. Zhang, Z. Y. Su, W. Li, M. T. Huang, and A. N. Kong, “The epigenetic effects of aspirin: the modification of histone H3 lysine 27 acetylation in the prevention of carcinogenesis process located at the colon in azoxymethane- and dextran sulfate sodium-treated CF-1 mice,” *Carcinogenesis* **37**, 616–624, doi: 10.1093/carcin/bgw042 (2016).
32. Z. L. Zhang, H. Y. Fan, M. Y. Yang, Z. K. Zhang, and K. Ke Liu, “Therapeutic effect of a hydroxynaphthoquinone fraction on dextran sulfate sodium-induced ulcerative colitis,” *World J Gastroenterol* **20**, 15310–15318, doi:10.3748/wjg.v20.i41.15310 (2014).
33. S. Takeda, H. Takeya, and S. Iwanaga, “Snake venom metalloproteinases: structure, function and relevance to the mammalian ADAM/ADAMTS family proteins,” *Biochim Biophys Acta* **1824**, 164–176, doi:
34. F. S. Markland, and S. Swenson, “Snake venom metalloproteinases,” *Toxicon* **62**, 3–18, doi: 10.1016/j.toxicon.2012.09.004 (2013).
35. L. A. Calderon, J. C. Sobrinho, K. D. Zaqueo, A. A. de Moura, A. N. Grabner, M. V. Mazzi, S. M. A. Nomizo, C. F. C. Fernandes, J. P. Zuliani, B. A. Carvalho, S. L. da Silva, R. G. Stábeli, and A. M. Soares, “Antitumoral activity of snake venom proteins: new trends in cancer therapy,” *BioMed Res Int*, **2014**, 203639, doi: 10.1155/2014/203639 (2014).
36. P. K. Akao, C. C. C. Tonoli, M. S. Navarro, A. C. O. Cintra, J. R. Neto, R. K. Arni, and M. T. Murakami, “Structural studies of BmooMP-alpha-I, a non-hemorrhagic metalloprotease from *Bothrops moojeni* venom,” *Toxicon* **55**, 361–368, doi: 10.1016/j.toxicon.2009.08.013 (2010).

Figure Legends

Figure 1. Macroscopic features at the colon. **A-** The experiment design of mice was induced Colitis by DSS administration. For the experiment, mice were divided into groups of six animals each, receiving the following inocula: **I**, sterile saline (vehicle, negative control); **II**, 50 µg BmooMP-alpha-I (positive control); **III**, DSS only (model group); **IV**, DSS plus BmooMP-alpha-I, at the doses of 50, 25, or 12.5 µg/ animal/day (treated group). At the end of 6 days, mice from all groups were euthanized and subject the clinical evaluation. **B-** Control group (without DSS), BmooMP-alpha-I (50 µg) group; 3% DSS administration group (DSS) and 3% DSS plus BmooMP-alpha-I (50 µg to 12.5 µg). **C-** Intestine length (cm). Data shown are expressed as mean ± SD ($n=6$ per group). Results represent means ± SD out of five analyses for each experimental condition. Comparisons were carried out by using one-way Anova and Dunnett's Multiple Comparison Test. $*p < 0.05$; $**p < 0.01$; ns: not significant in relation to the DSS or negative controls (Ctrl).

Figure 2. Effect of BmooMP-alpha-I on the clinical signs of mice in DSS induced colitis model. **A-** Clinical score; **B-** Post-mortem score; **C-** Accumulated score; **D-** Overall score. Results represent means ± SD out of five analyses for each experimental condition. Comparisons were carried out by using one-way Anova and Dunnett's Multiple Comparison Test. $*p < 0.05$; ns: not significant in comparison with the DSS group of animals.

Figure 3. Effect of BmooMP-alpha-I on cytokine production in DSS induced colitis. **A-** TNF, **B-** IFN-gamma and **C-** IL-12p40 concentration in supernatants of intestinal tissue homogenates. Results represent means ± SD out of five analyses for each experimental condition. Comparisons were carried out by using one-way Anova and Dunnett's Multiple Comparison Test. $*p < 0.05$; $**p < 0.01$; $***p < 0.001$; ns: not significant when compared with the DSS or negative control (Ctrl) groups.

Figure 4. Histological characteristics of colon from mice obtained at day 6 after induction of DSS colitis model in comparison with controls. H&E staining were performed on colon sections obtained from mice belonging to the following groups: **A-** Negative control group (no DSS); **B-** Positive control group (50 µg BmooMP-alpha-I); **C-** Model group (3% DSS); and **D-** Treated group (3% DSS + 50 µg BmooMP-alpha-I). Images were obtained at 10 x magnification in FSX100 Olympus Microscopy. The square demonstrates the loss of tissue architecture and

1 cell infiltration. The arrows indicate the goblet cells.
2

Figure 1

2

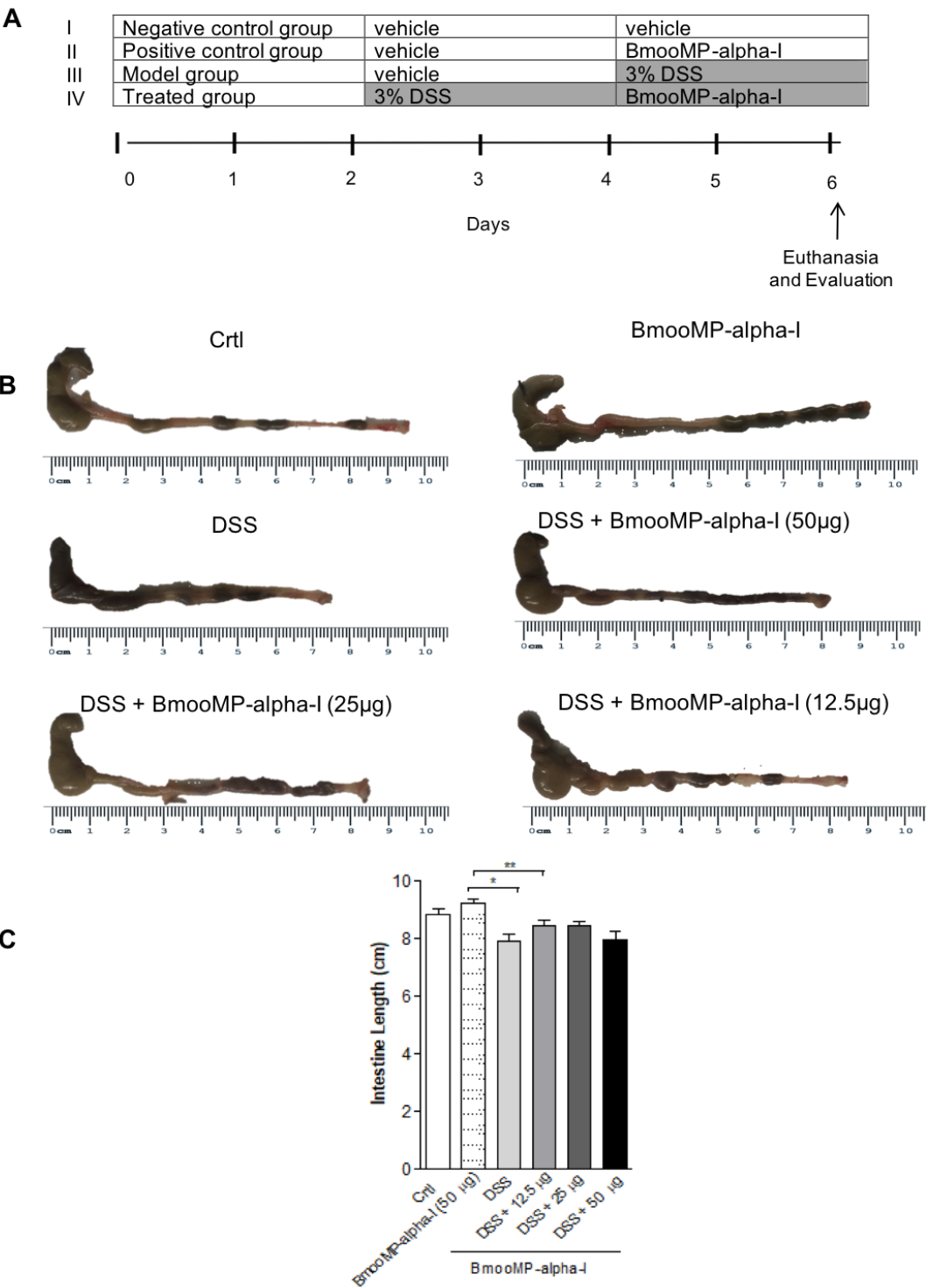


Figure 2

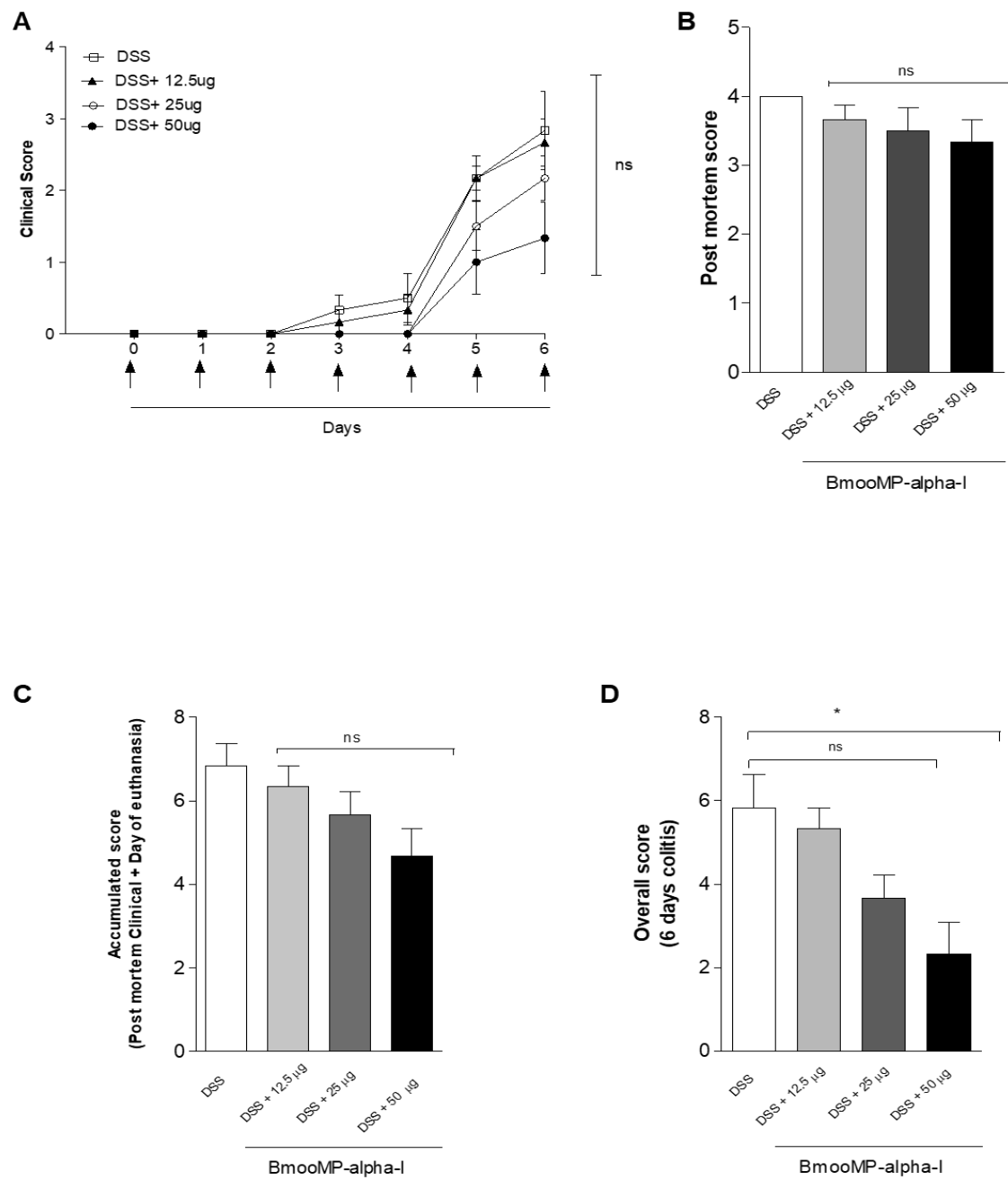


Figure 3

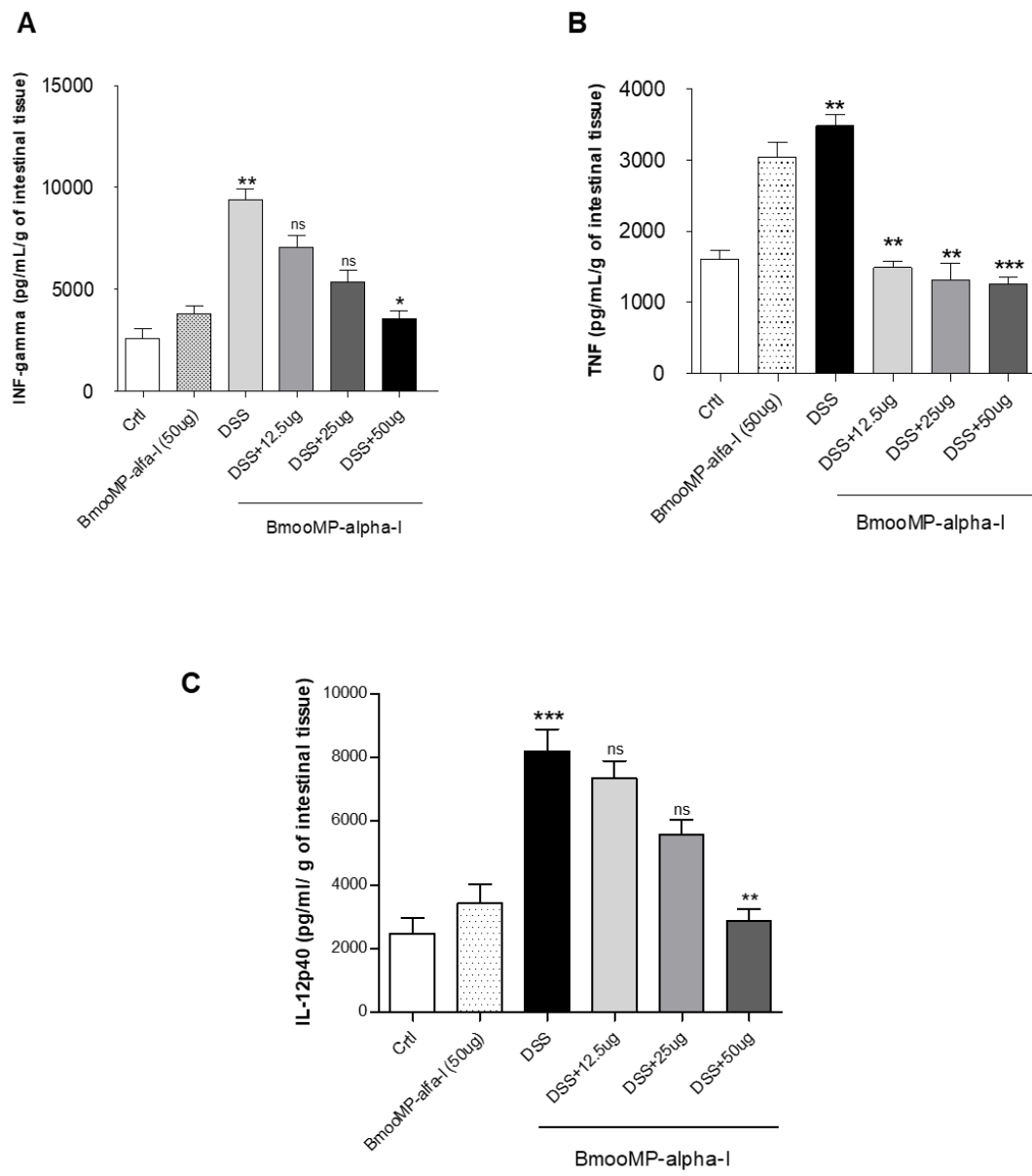
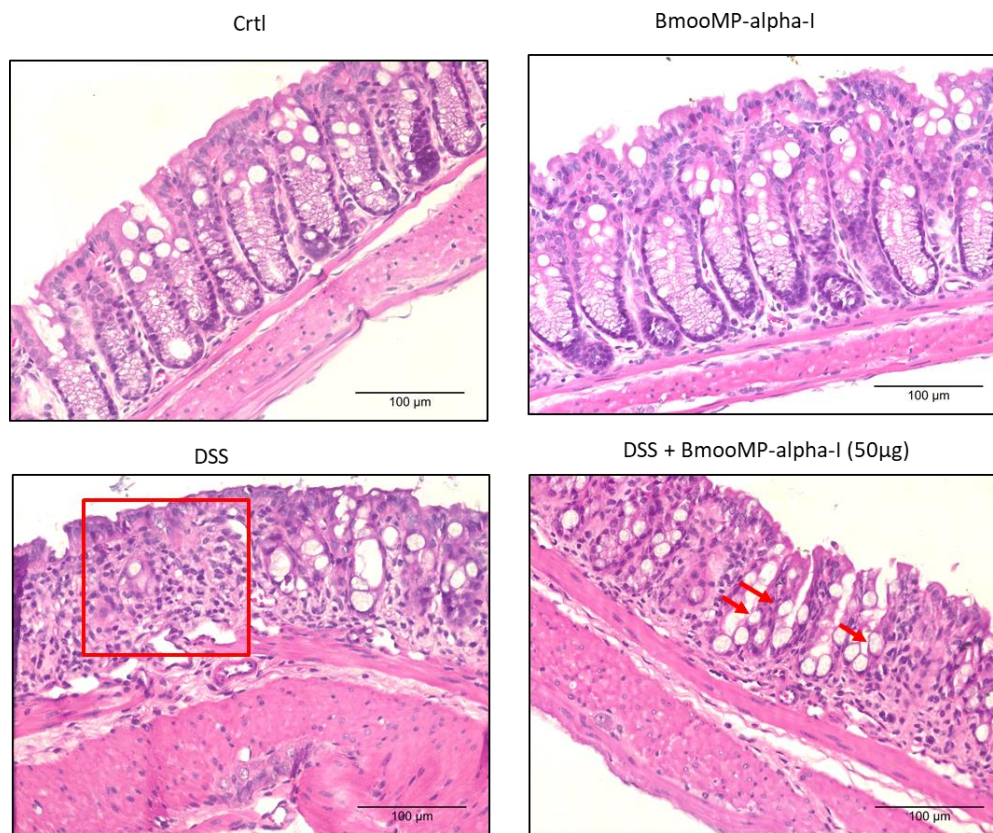


Figure 4



Capítulo III: PERPESCTIVAS FUTURAS

De acordo com os dados relatados na presente tese neste capítulo elucidaremos as propostas futuras para esta pesquisa com a finalidade de investigar como a metaloprotease BmooMP- α -I atua a nível molecular sobre TNF.

Neste sentido experimentos futuros serão realizados com o objetivo de determinar a especificidade de degradação de BmooMP- α -I nas ligações peptídicas formadas pelos aminoácidos das cadeias de TNF, de acordo com a seguinte metodologia:

- **Purificação da enzima BmooMP- α -I**

A metaloprotease BmooMP- α -I será purificada de acordo com o método descrito por Silva e colaboradores (2016). Cerca de 400 mg de peçonha bruta de *B. moojeni* serão dissolvidos em 4 mL de tampão bicarbonato de amônio (Sigma Chem. Co) a 50 mM (pH 7,8) e centrifugado a 10,000 x g por 10 min. A solução sobrenadante será cromatografada em coluna DEAE – Sephacel (Sigma Chem. Co) (1,7 x 15 cm), previamente equilibrada com tampão bicarbonato de amônio a 50 mM (pH 7,8) e eluída com um gradiente convexo/crescente de concentração (0,05-0,3 M) do mesmo tampão.

A segunda fração da cromatografia anterior, denominada E2, será ressuspensa em tampão bicarbonato de amônio a 50 mM, pH 7,8 e aplicada em uma coluna Sephadex – G75 (Amersham Pharmacia Ltda) (1 x 100cm) previamente equilibrada com o mesmo tampão. A segunda fração resultante da cromatografia de exclusão molecular (Sephadex G-75), denominada E2G2, será ressuspensa em 2 mL de tampão Tris-HCl 20 mM, pH 7,0 e aplicada em uma resina de Benzamidina Sepharose (Amersham Pharmacia Ltda) (20 X 15 cm). As amostras serão eluídas com tampão glicina 50 mM pH=3,0. As frações resultantes serão delimitadas e avaliadas quanto ao grau de pureza em eletroforese.

Todas as cromatografias serão realizadas coletando-se frações de 3,0 mL cada, com um fluxo de 20 mL/hora. A absorbância de cada fração será acompanhada em 280 nm no espectrofotômetro (Eppendorf Biophotometer plus), os gráficos serão construídos, as amostras selecionadas reunidas em “pools”, dosadas, liofilizadas e armazenadas a - 20°C até o momento de uso.

- **Dosagem de proteínas**

A concentração de proteínas da peçonha bruta e das frações isoladas será determinada pelo método de Bradford (1976), utilizando como proteína padrão a soroalbumina bovina (Sigma Chem. Co).

- **Eletroforese unidimensional (1D. SDS-PAGE)**

As eletroforeses em gel de poliacrilamida com agentes desnaturantes (SDS) serão realizadas conforme a técnica descrita por Laemmli, (1970) e servirá como critério de pureza da enzima BmooMP-alfa-I durante os passos de purificação.

- **Produção das proteínas recombinantes TNF e suas variantes mutantes**

A fim de determinar o possível ponto de clivagem de metaloprotease BmooMP-alfa-I na molécula de TNF, proteínas recombinantes de TNF solúvel (forma biologicamente ativa) e variações mutantes nos resíduos de aminoácidos de prolina que formam ligações peptídicas tipo p-p' nas posições 178,184, 191 e 195 serão clonadas em modelo procarioto. Desse modo, o cDNA para expressão proteica será obtido através do isolamento do RNA total de macrófagos peritoneais de camundongos C57BL/6 pelo método Trizol (Invitrogen, Carlsbad, EUA) segundo instruções do fabricante e a transcrição reversa das proteínas será desenvolvida utilizando os primers adequados. O produto da reação será clonado em vetor de expressão com gene de resistência a antibiótico e calda de histidina na porção C-terminal para purificação.

E. coli da cepa BL21DE competente será preparadas para posterior inserção do plasmídeo. Brevemente, as bactérias serão crescidas em meio Luria e Bertani (LB), centrifugadas, ressuspendidas em Cloreto de Cálcio (CaCl_2) e incubadas a 0°C por uma hora. A transformação bacteriana ocorrerá com a adição de DNA plasmidial. Posteriormente, as bactérias serão incubadas a 42°C durante duas horas e colocadas novamente na condição anterior. Será adicionado o meio de cultura LB por uma hora. Após incubação, as células serão centrifugadas e o *pellet* ressuspendido em meio LB com o antibiótico de seleção e clonafenicol e as bactérias serão plaqueadas em placas de ágar para

análise de colônias transformadas. Além disso, o DNA plasmidial será isolado de cada uma das colônias crescentes e avaliado por PCR.

Bactérias transformadas serão crescidas em meio LB com antibiótico e clonafenicol para crescimento. A expressão proteica será induzida com isopropil- β -D-tiogalactosídeo (IPTG). A indução será avaliada em gel de eletroforese SDS-PAGE e *Western blotting*. Colônias de bactérias expressando as proteínas de interesse serão centrifugadas e o *pellet* será ressuspensionado em tampão de lise e mantidos em banho de gelo durante 30 minutos. Posteriormente, as bactérias serão submetidas a seis ciclos de congelamento em N₂ líquido e descongelamento a 37°C e posteriormente por ciclos de ultrassom. O lisado será centrifugado e o sobrenadante será passado em coluna Ni²⁺ *chelating sepharose* (GE Biosciences Amersham, NLD) com tampão de equilíbrio. Após aplicação do material, a coluna será lavada e as proteínas serão eluídas com tampão fosfato com imidazol.

- **Ensaio enzimático**

A atividade proteolítica da enzima BmooMP-alfa-I sobre o substrato TNF será realizada segundo Wang e colaboradores (2008), com modificações. Em 1mL de solução contendo serão diluídos TNF em PBS estéril serão adicionados a enzima BmooMP-alfa-I e incubados por 1h a 37°C (proporção 0,7 ng de TNF para 12 μ g de BmooMP-alfa-I). Como controle negativo, será realizada a incubação de TNF somente com PBS estéril. Os produtos de degradação do substrato resultante do ensaio enzimático serão submetidos à eletroforese bidimensional em condições desnaturantes (2D-SDS.PAGE). Após a corrida, os géis serão retirados da placa e mergulhados em uma solução corante contendo Coomassie Brilliant Blue R-250 0,2% (m/v) em água-metanol-ácido acético (4:5: 1 v/v) por 10 minutos. Em seguida, os géis serão descorados por uma solução de água e ácido acético 7% (v/v).

- **Identificação do ponto de clivagem de BmooMP-alfa-I na citocina TNF**

Após a coloração do gel, os spots marcados derivados dos produtos da degradação enzimática serão excisados do gel e sequenciados por degradação de Edman. A sequência de aminoácidos hidrolisados será determinada por análise *in silico* em alinhamentos múltiplos por meio da plataforma Clustalw2: (<http://www.ebi.ac.uk/Tools/msa/clustalw2/>). Posteriormente por análise da sequência primária total de TNF será determinado às ligações peptídicas preferencialmente hidrolisadas por BmooMP-alfa-I.

Tal conhecimento pode ser útil para o desenvolvimento de um protótipo para o desenvolvimento de novos fármacos para o tratamento de desordens pró- inflamatórias.

A metaloprotease BmooMP-alfa-I possui um mecanismo de ação distinto dos inibidores de TNF (TNFIs), a mesma realiza uma proteólise sobre a citocina pró-inflamatória TNF em sua forma solúvel, como demonstrado nos ensaios *in vitro* e *in vivo*.

A indústria farmacêutica desenvolve produtos farmacêuticos derivados de componentes ativos obtidos por síntese química e outros sintetizados por organismos vivos, principalmente proteínas e/ou um ácido nucléicos são os chamados biofármacos. A estrutura molecular dos biofármacos é extremamente complexa, pois o componente ativo é uma biomolécula heterogênea. Estas biomoléculas são difíceis de caracterizar e de replicar. Os biofármacos são elaborados utilizando matéria-prima procedente de duas origens, o componente ativo de origem biológica, que são extraídos de microorganismos, órgãos e tecidos de origem vegetal ou animal, células ou fluidos de origem humana ou animal; ou componente ativo de origem biotecnológica, em geral, são proteínas obtidas a partir de células modificadas geneticamente para produzi-las.

Os compostos farmacêuticos produzidos a partir da peçonha de serpentes são biofármacos de origem biológica derivados de proteínas isolados a partir da mesma, ou como moléculas análogas a estas proteínas ou até mesmo peptídeos sintetizados a partir de estrutura molecular destes compostos. As biomoléculas isoladas da peçonha de serpentes são protótipos para produção de novos fármacos e a compreensão de diversos fenômenos biológicos.

Portanto, estes estudos estruturais irão auxiliar na compreensão do mecanismo de ação biológica da enzima BmooMP- α -I e na proposta do design de um novo fármaco com ação anti-inflamatória.